Variation in *CFHR3* determines susceptibility to meningococcal disease by controlling factor H concentrations

Authors

Vikrant Kumar, Richard B. Pouw, Matias I. Autio, ..., Michael Levin, Taco W. Kuijpers, Sonia Davila

Correspondence

t.w.kuijpers@amsterdamumc.nl (T.W.K.), gmssmdd@nus.edu.sg (S.D.)

Neisseria meningitidis **evades complement-mediated clearance by hijacking host complement regulator factor H (FH). Kumar et al. investigate the genetic variations in the *CFH* locus associating with meningococcal disease. A regulatory region in the adjacent *CFHR3* gene controls *CFH* expression, thereby determining FH plasma amounts and susceptibility towards meningococcal disease.**

Kumar et al., 2022, The American Journal of Human Genetics *109*, 1680–1691
September 1, 2022

https://doi.org/10.1016/j.ajhg.2022.08.001

CellPress

ARTICLE

Variation in *CFHR3* determines susceptibility to meningococcal disease by controlling factor H concentrations

Vikrant Kumar,[1,2,35] Richard B. Pouw,[3,4,5,35] Matias I. Autio,[1,6,35] Manfred G. Sagmeister,[7,35] Zai Yang Phua,[1] Lisa Borghini,[1,26,27] Victoria J. Wright,[8] Clive Hoggart,[8,34] Bangfen Pan,[1,6] Antson Kiat Yee Tan,[9] Alexander Binder,[7] Mieke C. Brouwer,[4,5] Ellie Pinnock,[10] Ronald De Groot,[11] Jan Hazelzet,[12] Marieke Emonts,[13,14,15] Michiel Van Der Flier,[11,16] Karl Reiter,[17] Markus M. Nöthen,[18] Per Hoffmann,[18] EUCLIDS consortium, Luregn J. Schlapbach,[19,20,21] Evangelos Bellos,[8] Suzanne Anderson,[22] Fatou Secka,[22] Federico Martinón-Torres,[23,24,25] Antonio Salas,[25,26,27] Colin Fink,[10] Enitan D. Carrol,[28] Andrew J. Pollard,[29] Lachlan J. Coin,[30] Werner Zenz,[7] Diana Wouters,[4,5] Lay Teng Ang,[9] Martin L. Hibberd,[31,32] Michael Levin,[8,36] Taco W. Kuijpers,[3,36,*] and Sonia Davila[1,2,33,36,*]

Summary

Neisseria meningitidis protects itself from complement-mediated killing by binding complement factor H (FH). Previous studies associated susceptibility to meningococcal disease (MD) with variation in *CFH*, but the causal variants and underlying mechanism remained unknown. Here we attempted to define the association more accurately by sequencing the *CFH-CFHR* locus and imputing missing genotypes in previously obtained GWAS datasets of MD-affected individuals of European ancestry and matched controls. We identified a *CFHR3* SNP that provides protection from MD (rs75703017, p value = 1.1×10^{-16}) by decreasing the concentration of FH in the blood (p value = 1.4×10^{-11}). We subsequently used dual-luciferase studies and CRISPR gene editing to establish that deletion of rs75703017 increased FH expression in hepatocyte by preventing promotor inhibition. Our data suggest that reduced concentrations of FH in the blood confer protection from MD; with reduced access to FH, *N. meningitidis* is less able to shield itself from complement-mediated killing.

Introduction

Meningitis and sepsis caused by *Neisseria meningitidis* remain amongst the most feared bacterial infections world-wide. Although immunization has decreased the incidence of invasive meningococcal disease (MD) in some countries, there are no vaccines effective against all serogroups, and the emergence of new serogroups and

[1]Human Genetics, Genome Institute of Singapore, Singapore, Singapore; [2]Duke-National University of Singapore Medical School, Singapore, Singapore; [3]Division of Pediatric Immunology, Rheumatology, and Infectious Diseases, Emma Children's Hospital, Amsterdam University Medical Centre, Amsterdam, the Netherlands; [4]Department of Immunopathology, Sanquin Research, Amsterdam, the Netherlands; [5]Landsteiner Laboratory, Amsterdam University Medical Centre, Amsterdam Infection and Immunity Institute, Amsterdam, the Netherlands; [6]Cardiovascular Research Institute, Centre for Translational Medicine, National University Health System, Singapore; [7]Department of General Paediatrics, Medical University of Graz, Graz, Austria; [8]Section of Paediatric Infectious Disease, Division of Infectious Disease, Department of Medicine, Imperial College London, London, UK; [9]Cancer Stem Cell Biology, Genome Institute of Singapore, Singapore, Singapore; [10]Micropathology, University of Warwick, Coventry, UK; [11]Section of Pediatric Infectious Diseases, Laboratory of Medical Immunology, Department of Laboratory Medicine, Radboud Institute for Molecular Life Sciences, Radboud University Medical Center, Nijmegen, The Netherlands; [12]Department of Pediatrics, Erasmus Medical Center-Sophia Children's Hospital, University Medical Center, Rotterdam, the Netherlands; [13]Translational and Clinical Research Institute, Newcastle University, Newcastle Upon Tyne, UK; [14]National Institute for Health and Care Research Newcastle Biomedical Research Centre Based at Newcastle Upon Tyne Hospitals National Health Service Trust and Newcastle University, Newcastle Upon Tyne, UK; [15]Paediatric Infectious Diseases and Immunology Department, Newcastle Upon Tyne Hospitals Foundation Trust, Great North Children's Hospital, Newcastle Upon Tyne, UK; [16]Paediatric Infectious Diseases and Immunology, Wilhelmina Children's Hospital University Medical Centre Utrecht, Utrecht, the Netherlands; [17]Department of Paediatrics, Division of Paediatric Intensive Care Medicine, Ludwig Maximilian University of Munich and Dr. von Hauner's Children's Hospital, Munich, Germany; [18]Institute of Human Genetics, University of Bonn, Bonn, Germany; [19]Child Health Research Centre, The University of Queensland, Brisbane, Australia; [20]Paediatric Intensive Care Unit, Queensland Children's Hospital, Brisbane, Australia; [21]Department of Intensive Care and Neonatology and Children's Research Center, University Children's Hospital Zurich, Zurich, Switzerland; [22]Medical Research Council Unit Gambia, Banjul, The Gambia; [23]Translational Pediatrics and Infectious Diseases, Hospital Clínico Universitario de Santiago, Santiago de Compostela, Spain; [24]Genetics, Vaccines, Infectious Diseases, and Pediatrics Research Group, Instituto de Investigación Sanitaria de Santiago, Universidad de Santiago de Compostela, Santiago de Compostela, Spain; [25]Centro de Investigación Biomédica en Red de Enfermedades Respiratorias, Instituto de Salud Carlos III, Madrid, Spain; [26]Unidade de Xenética, Instituto de Ciencias Forenses, Facultade de Medicina, Universidade de Santiago de Compostela, Santiago de Compostela, Spain; [27]GenPoB Research Group, Instituto de Investigación Sanitaria de Santiago, Hospital Clínico Universitario de Santiago, Santiago de Compostela, Spain; [28]Institute of Infection, Veterinary and Ecological Sciences, University of Liverpool, Liverpool, UK; [29]Oxford Vaccine Group, Department of Pediatrics, University of Oxford and the NIHR Oxford Biomedical Research Centre, Oxford, UK; [30]Department of Microbiology and Immunology, The Peter Doherty Institute for Infection and Immunity, University of Melbourne, Melbourne, VIC, Australia; [31]Infectious Diseases, Genome Institute of Singapore, Singapore, Singapore; [32]Infectious and Tropical Disease, London School of Hygiene & Tropical Medicine, London, UK; [33]SingHealth Duke-NUS Institute of Precision Medicine, Singapore, Singapore
[34]Present address: Department of Genetics and Genomic Sciences, Icahn School of Medicine at Mount Sinai, New York, NY, USA
[35]These authors contributed equally
[36]These authors contributed equally
*Correspondence: t.w.kuijpers@amsterdamumc.nl (T.W.K.), gmssmdd@nus.edu.sg (S.D.)
https://doi.org/10.1016/j.ajhg.2022.08.001.

strains[1,2] poses new challenges to international vaccination strategies. Epidemics and outbreaks continue to occur in many countries, particularly in the meningitis belt of sub-Saharan Africa.[3–6]

A remarkable feature of *N. meningitidis* is that it is a harmless commensal for the majority of the world's population and is carried in the nasopharynx repeatedly throughout life. Invasive disease occurs in 0.16–20 per 100,000 people in developed countries, but there is wide variation in incidence, and epidemics occur.[1,2,7,8]

There is good evidence that genetic factors play a role in MD.[9–11] Rare Mendelian defects in complement genes are associated with familial MD.[12,13] Our previous genome-wide association study (GWAS) identified an association between MD and a broad genomic region spanning complement factor H (*CFH* [MIM: 134370]) and the complement factor H-related protein (in genetic order; *CFHR3* [MIM: 605336], *CFHR1* [MIM: 134371], *CFHR4* [MIM: 605337], *CFHR2* [MIM: 600889], and *CFHR5* [MIM: 608593]) genes.[10] Identification of the causal gene and characterization of the functional variant(s) have been difficult because of the complexity of the region; *CFH* shows sequence similarity to the five adjacent *CFHR* genes on human chromosome 1.[14]

Factor H (FH) is a serum glycoprotein that is synthesized mostly in the liver and acts as a negative regulator of the alternative complement activation pathway.[15] FH is a crucial factor in preventing host cell damage by uncontrolled complement activation,[16] and genetic variation in *CFH* or the *CFHR* genes is associated with several diseases, including systemic lupus erythematosus (SLE [MIM: 152700]),[17] glomerulonephritis,[18] IgA nephropathy,[19] atypical hemolytic uremic syndrome (aHUS [MIM: 235400])[20] and age-related macular degeneration (AMD [MIM: 603075]),[21,22] although the mechanistic process leading to disease is unclear for all these diseases.

N. meningitidis expresses several membrane proteins that bind human FH; Neisserial surface protein A (NspA),[23] Porin B2 (PorB2),[24] Porin B3 (PorB3),[25] and FH-binding protein (fHbp)[26] and is believed to survive and replicate in human blood by using the surface bound FH in a "Trojan horse" process to inhibit complement-mediated killing. Genetically regulated differences in FH plasma concentrations might thus alter susceptibility to *N. meningitidis*. Furthermore, inhibition of complement by "hijacking" FH has been adopted as an immune evasion strategy by several pathogens, including fungi, parasites, and viruses next to bacteria (reviewed in[27]). We aimed to identify the mechanism underlying the association of variants within the *CFH-CFHR* region with susceptibility and resistance to MD.

Methods

Study sample sets

The design for our study and the composition of clinical cohorts are shown in Figure S1 and Table S1. Clinical details of individuals with MD in UK, Spanish, and other European cohorts have been reported previously, as have the diagnostic criteria, recruitment procedure, and ethical approvals[10,28] (supplementary Appendix). 238 individuals with MD and 237 controls from the Central European cohort (CEC) were used for deep sequencing the *CFH-CFHR* region. Replication of the most significant SNPs was undertaken in 1,522 individuals with MD and 2,672 controls (755 individuals with MD and 1,253 controls from the UK, 279 individuals with MD and 395 controls from Central Europe, and 488 individuals with MD and 1,024 controls from Spain).[10,11] Previously genome-wide-genotyped cohorts totaling 1,246 individuals with MD and 7,197 controls (472 individuals with MD and 4,614 controls from the UK; 358 individuals with MD and 1,770 controls from Central Europe;[29] and 416 individuals with MD and 813 controls from Spain[9,10]) were newly imputed, and the data were used for a subsequent meta-analysis. Convalescent serum was available from 367 individuals with MD (308 UK, 59 Dutch) and 124 healthy, unrelated Dutch controls for measurement of FH and FHR-3 concentrations; of the 308 UK individuals with MD, 295 were included in protein quantitative trait loci (pQTL) analysis, together with 56 healthy, unrelated controls from Central Europe.

Sequencing and genotyping of the *CFH-CFHR* region

To identify functional variants driving the association with MD susceptibility, we devised a capture-targeted sequencing strategy with tiling arrays (designed by Roche NimbleGen) covering more than 85% of the *CFH-CFHR* region spanning 359 kb on chromosome 1 (chr1: 196,620,000–196,979,000, GRCh37/hg19) and then performed sequencing with Illumina HiSeq 2000 by using 100 bp paired-end reads (stage 1, see supplemental information). The average depth of sequencing was 227× (Figure S2). We validated the most significant SNPs (stage 2, see supplemental information) by using a Sequenom Multiplex MassArray (San Diego, USA).

Genetic association testing was carried out with Fisher's exact test for rare SNPs (MAF $< 1\%$) and logistic regression analysis for common SNPs and copy-number variants (CNVs) under an additive genetic model. To mitigate the effect of population stratification, we analyzed association of SNPs with MD separately in all three replication cohorts under the additive model and performed meta-analysis for both SNPs and CNVs by combining summary statistics of stage 1 (deep sequencing) and stage 2 (Sequenom validation) by using the Cochran-Mantel-Haenszel (CMH) test. For CNVs, all samples were combined and analyzed under a genotypic and additive model.

Detection of copy-number variation

CNVs were detected in the resequencing dataset (238 individuals with MD and 237 controls from Central Europe) with cnvCapSeq (version 0.1.230) and cross-validated by quantitative PCR in the same cohort (Taqman qPCR, Table S2). In the second-stage validation of the 51 SNPs across the Central Europe, UK, and Spanish cohorts, detection of CNVs was done with the Taqman qPCR assays. For pQTL data, multiplex ligation-dependent probe amplification (MLPA) and Taqman assays were used for identifying CNVs (supplemental information).

Genotype-phenotype correlation of SNPs and CNVs were analyzed for FH and FHR-3 concentrations via linear regression analysis. We used ANCOVA, with sex as a covariate, to estimate the overall difference in the protein concentrations across six genotype groups. Differences in protein concentrations between two genotype groups were evaluated by t test.

Imputation of genome-wide genotyped data

To confirm our resequencing analysis by using current genome assemblies, we re-analyzed our original UK GWAS data,[10] including newly genome-wide-genotyped cohorts from Central Europe[29] and Spain[11] (stage 3, see supplemental information). After pre-processing (supplemental information), we used BEAGLE (version 5.1[30]) to perform haplotype estimation and imputation of missing genotypes by utilizing alternately the Haplotype Reference Consortium (HRC [http://www.haplotype-reference-consortium.org]; HRC release 1.1 [https://ega-archive.org/datasets/EGAD00001002729]) and the 1000 Genomes Project phase 3 (1KGP [http://www.internationalgenome.org]) as reference genomes.

After extraction of the individually calculated allele dose, which is the sum of the two allele probabilities based on a hidden Markov model, we applied a univariate linear mixed-model algorithm (uLMM) using a centered relatedness matrix implemented in GEMMAsoftware (version 0.98.1[31]) to perform genetic association testing for quantitative traits under an additive model. To additionally account for population stratification, we used the first two or four principal components (PCs; Figure S4) as covariates in each individual cohort. Furthermore, the genomic control function implemented in the GWAMA software (version 2.2.2[32]) was used for the subsequent meta-analysis of the single summary statistics, resulting in an overall genomic control lambda (λ_{GC}) of 1.002 (95% CI 0.094–1.010) when all variants were used and 1.007 (95% CI 0.971–1.0432) when only genotyped variants were used (Figure S5).

Serum concentrations of FH and FHR-3

FH and FHR-3 concentrations were determined by specific ELISAs as previously described.[33] In brief, the antigen was captured with monoclonal antibody anti-FH.16 and anti-FHR-3.1 for FH and FHR-3, respectively (Sanquin Research, Amsterdam, The Netherlands). Bound FH was subsequently detected by the use of polyclonal goat anti-human FH antibodies, and bound FHR-3 was detected with monoclonal anti-FHR-3.4 (Sanquin Research).

Differentiation of human embryonic stem cells

Wild-type and CRISPR/Cas-targeted H1 human embryonic stem (hES) cells were differentiated to hepatocyte-like cells over 18 days as previously described.[34]

Genome editing of differentiated hepatocytes by CRISPR/Cas9

Guide RNAs flanking the liver-specific regulatory region of interest in *CFHR3* were designed, incorporated in plasmids, and transfected via electroporation into H1 hES cells (Table S3). After incubation for two days, Clover^{+} cells were seeded at 500–1,000 cells per well of a 6-well plate. After 2-3 weeks culture, single colonies were picked and expanded for screening. Deletion of liver specific regulatory region was determined by PCR with primers spanning the targeted region (Table S3). Confirmed deletion clones and wild-type controls were used for detecting RNA expression by RT-PCR (see supplemental information).

Results

Fine mapping of the *CFH-CFHR* region identifies *CFHR3* as the lead association

Deep sequencing of the *CFH-CFHR* region in 238 individuals with MD and 237 healthy controls identified 4,369 SNPs after application of stringent quality-control filters (Table S4). The strongest signal of association was identified on *CFHR3* in a region with high linkage disequilibrium (LD, D′ = 0.92) with the previously reported lead variant, rs1065489 in *CFH*.[10,11,35] The 51 SNPs with the strongest association with MD were selected for validation, and 44 SNPs were successfully typed (Table S5) in the UK, Spanish, and Central European cohorts (n = 4,194). 13 SNPs, in a tight LD block within *CFHR3*, achieved genome-wide significance in the meta-analysis (Figure 1, Table 1), confirming the genetic association with *CFHR3*. The lead SNP (Table 1), rs75703017 (p value = 1.1×10^{-16}), located in intron 1 of *CFHR3*, showed consistent odds ratios (OR = 0.62) for susceptibility to MD in all cohorts, indicating a protective effect (Figure 2).

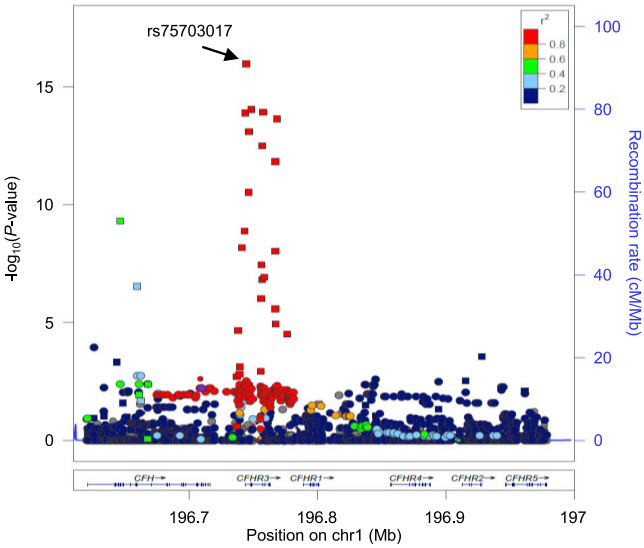

Figure 1. Fine mapping by sequencing of the *CFH-CFHR* locus
Plot showing association results of all the SNPs (arranged according to their GRCh37/hg19 build chromosomal position on the x axis) from deep sequencing (circle) and from meta-analysis (square) with combined stage 1 and stage 2 cohorts. The top SNP from the analysis is labeled (rs75703017). The color intensity of each symbol reflects the extent of LD with the top GWAS SNP.

Imputation across the *CFH-CFHR* region confirms a broad region of association

Imputation of genome-wide genotyped data in three different European cohorts including 1,246 individuals with MD and 7,197 controls was complicated by the reported CNVs nsv3888824 (deletion) spanning 84,671 bases and resulting in a hybrid *CFH/CFHR1* gene and nsv4649133 (deletion) spanning 79,989 bases and resulting in a complete deletion of *CFHR3* and *CFHR1* (Figure 3C). Using a subset of the HRC reference panel identified only four of the 13 SNPs found within and adjacent to *CFHR3* by our resequencing work, whereas use of the 1KGP reference panel, which identified 11 SNPs with high confidence in a tight LD block closely around the genome-wide significance level of 5×10^{-8} (Table 2 and Figure 3). The usage of updated references and bioinformatic tools for the association mapping

Table 1. Unadjusted p values and ORs of top SNPs from sequencing, genotyping, and the combined analysis

	Sequence				Replication													
	Central Europe				Central Europe				UK				Spain				Combined CMH[a]	
SNP ID	MAF MD	MAF con	p value	OR	MAF MD	MAF Con	p value	OR	MAF MD	MAF con	p value	OR	MAF MD	MAF Con	p value	OR	p value	OR
rs75703017	0.12	0.21	3.11×10^{-3}	0.62	0.14	0.21	3.60×10^{-3}	0.68	0.14	0.21	8.34×10^{-6}	0.71	0.18	0.26	2.26×10^{-4}	0.72	1.11×10^{-16}	0.62
rs620015	0.13	0.21	6.18×10^{-3}	0.65	0.14	0.22	3.62×10^{-3}	0.68	0.15	0.21	2.27×10^{-5}	0.73	0.20	0.26	1.01×10^{-3}	0.75	9.55×10^{-15}	0.64
rs387107	0.14	0.21	9.35×10^{-3}	0.67	0.14	0.21	4.49×10^{-3}	0.68	0.15	0.21	4.97×10^{-5}	0.74	0.20	0.27	3.11×10^{-4}	0.73	1.24×10^{-14}	0.65
rs385390	0.14	0.22	6.04×10^{-3}	0.65	0.15	0.22	9.74×10^{-3}	0.71	0.15	0.21	1.50×10^{-5}	0.72	0.20	0.27	7.11×10^{-4}	0.75	1.35×10^{-14}	0.65
rs12409571	0.13	0.21	5.04×10^{-3}	0.64	0.14	0.21	8.20×10^{-3}	0.70	0.15	0.20	1.10×10^{-4}	0.75	0.19	0.26	2.46×10^{-4}	0.73	2.38×10^{-14}	0.65
rs425524	0.13	0.21	7.46×10^{-3}	0.65	0.36	0.45	4.97×10^{-3}	0.73	0.31	0.42	2.63×10^{-9}	0.66	0.46	0.50	9.96×10^{-2}	0.87	8.26×10^{-14}	0.69
rs401188	0.13	0.21	5.98×10^{-3}	0.65	0.22	0.25	3.36×10^{-1}	0.87	0.20	0.34	1.14×10^{-13}	0.46	0.34	0.38	3.22×10^{-2}	0.76	3.32×10^{-13}	0.64
rs1738741	0.14	0.21	9.35×10^{-3}	0.67	0.14	0.21	1.06×10^{-2}	0.71	0.15	0.21	1.39×10^{-5}	0.72	0.22	0.27	1.43×10^{-2}	0.81	1.54×10^{-12}	0.67
rs376841	0.13	0.21	4.42×10^{-3}	0.64	0.10	0.16	1.55×10^{-3}	0.56	0.10	0.15	1.29×10^{-5}	0.63	0.14	0.18	4.74×10^{-4}	0.65	3.06×10^{-11}	0.66
rs1329423	0.19	0.27	4.10×10^{-3}	0.63	0.21	0.26	3.43×10^{-2}	0.75	0.21	0.25	9.72×10^{-4}	0.78	0.23	0.30	7.31×10^{-5}	0.70	5.07×10^{-10}	0.73
rs11807997	0.13	0.21	5.12×10^{-3}	0.64	0.19	0.18	8.97×10^{-1}	1.02	0.15	0.21	1.24×10^{-4}	0.74	0.19	0.25	1.12×10^{-3}	0.75	1.34×10^{-9}	0.71
rs12408446	0.13	0.20	7.96×10^{-3}	0.65	0.20	0.18	5.19×10^{-1}	1.08	0.15	0.21	8.96×10^{-5}	0.74	0.19	0.25	1.36×10^{-3}	0.76	6.86×10^{-9}	0.72
rs116249058	0.14	0.21	7.53×10^{-3}	0.66	0.12	0.14	2.54×10^{-1}	0.83	0.12	0.15	1.74×10^{-2}	0.81	0.14	0.21	8.85×10^{-5}	0.67	9.59×10^{-9}	0.70

[a]CMH = Cochran-Mantel-Haenszel test; MD = individuals with meningococcal disease; con = healthy controls; MAF = minor-allele frequency; OR = odds ratio.

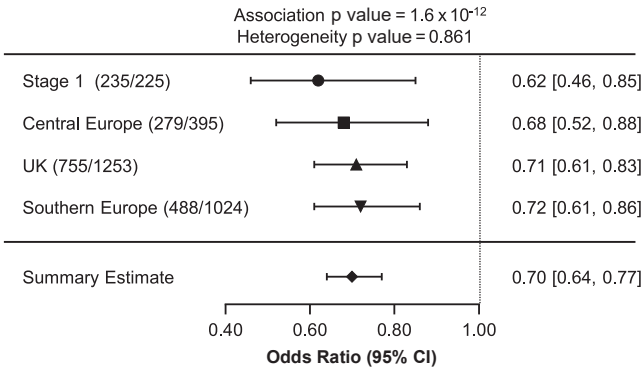

Figure 2. Forest plot of the top SNP, rs75703017
Plot showing odds ratios (ORs) and confidence intervals in each of the four cohorts; the summary estimate is shown below. The dotted vertical line indicates no effect. Cohort names with numbers of MD individuals and healthy controls are on the left, ORs and 95% CI are on the right.

(Figure 3) allowed us to impute variants within the complex region in and adjacent to *CFHR3*, but we were still unable to refine the location of the causative variant within the *CFH-CFHR* locus as a result of the apparent tight LD. Indeed, we observed discrepancies between the FH associations reported by Sun et al.[36] and our findings based on the 1KGP controls (Table S6); we suspect these discrepancies are due to differences in the imputation methods used for estimating the CNVs. Using imputation for the CNVs, we found peak association with MD outside the CNVs; whreas direct measurement of the CNVs shows the peak association to be within them (Figure 1).

Serum concentrations of FH, but not FHR-3, are lower in controls than in individuals who survived MD

To explore the relationship between serum concentrations of FH, FHR-3, and MD, we measured concentrations in serum from individuals who survived invasive MD, at least six months after the acute illness. Serum concentrations of FH were significantly lower in healthy controls than in those with MD (Figure 4A). In contrast, FHR-3 serum concentrations were not significantly different between MD survivors and controls (Figure 4A).

Low serum concentrations of FH are associated with both SNPs and CNVs in *CFHR3*

To investigate the effect of the top associated SNPs on the serum concentrations of FH and FHR-3, we undertook pQTL analysis, relating protein concentrations and genotype. The minor allele (A) of the lead SNP (rs75703017), shown to confer protection against MD (OR = 0.63), also showed the most significant association with lower FH serum concentrations ($p = 1.4 \times 10^{-11}$, Figure 4B), as confirmed in a pairwise comparison between genotypes carrying the minor allele (A) of rs75703017 (Figures 4B and 4C and Tables S7 and S11).

A common deletion spanning *CFHR3* and *CFHR1* (including rs75703017) has been shown to influence susceptibility to several inflammatory diseases.[17,19,21,37] To establish whether this deletion was also associated with susceptibility to MD, we determined CNVs in the sequenced individuals with MD by using cnvcapSeq,[38] which permits detection of CNVs in long-range targeted sequencing data. We then validated the findings by MLPA or qPCR analysis in a subset of samples (1,302 individuals with MD, 1,463 controls) from three European cohorts. Meta-analysis of CNV data revealed an overall lack of association ($p = 0.76$) between the *CFHR3/CFHR1* deletion and susceptibility to MD (Table S8), as previously reported.[10,35] Considering that the pQTL data indicated a dominant effect of the minor allele (A) of rs75703017, we performed a second comparison consisting of minor-allele carriers (A) vs. *CFHR3/CFHR1* deletion allele carriers. In contrast to the initial overall lack of association, this second comparison revealed that deletion of *CFHR3/CFHR1* was in fact associated with higher genetic risk of MD ($p = 0.0081$, Table S9) and increased FH serum concentrations. This positive genetic association with the *CFHR3/CFHR1* deletion was only detected when the combination of three alleles (wild type allele C, minor allele A, and deletion D) in rs75703017 were taken into account. Meta-analysis of the quantitative-trait association removing all samples with the *CFHR3/CFHR1* deletion did not modify the results (Figure S3), indicating that the association of rs75703017 persists regardless of *CFHR3/CFHR1* deletion status (Table S11).

CFHR3 controls *CFH* expression through epigenetic long-range interaction

Having established the correlation between "protective genotypes" and lower serum concentrations of FH and between "risk genotypes" and higher concentrations of FH, we next investigated the epigenetic histone marks in various cell lines to provide information on the putative regulatory role of the potential functional SNP in *CFHR3*. Histone marks (H3K4me3 and H3K9ac) from the Roadmap epigenomics database indicated that all investigated hepatic cell lines have an active regulatory site within *CFHR3*. Furthermore, no other cell types (non-hepatic) tested showed any indication of regulatory regions, suggesting that this functional site might be specifically active in liver cells,[39,40] which is concordant with the liver's being the main FH-producing organ.[14] In line with our hypothesis that there is a regulatory interaction between *CFHR3* and *CFH*, we examined whether the homozygous deletion of *CFHR3/CFHR1*, carried by 3% of the European population, affected FH protein concentrations. Indeed, the deletion of *CFHR3/CFHR1*, identified by the lack of FHR-3 in serum, was associated with significantly higher FH protein concentrations (Figure 4B).

Dual-luciferase assays confirm liver-specific activity

To confirm the role of the rs75703017 minor allele identified in our fine mapping in regulating *CFH* activation, we compared luciferase activity of a liver cell line

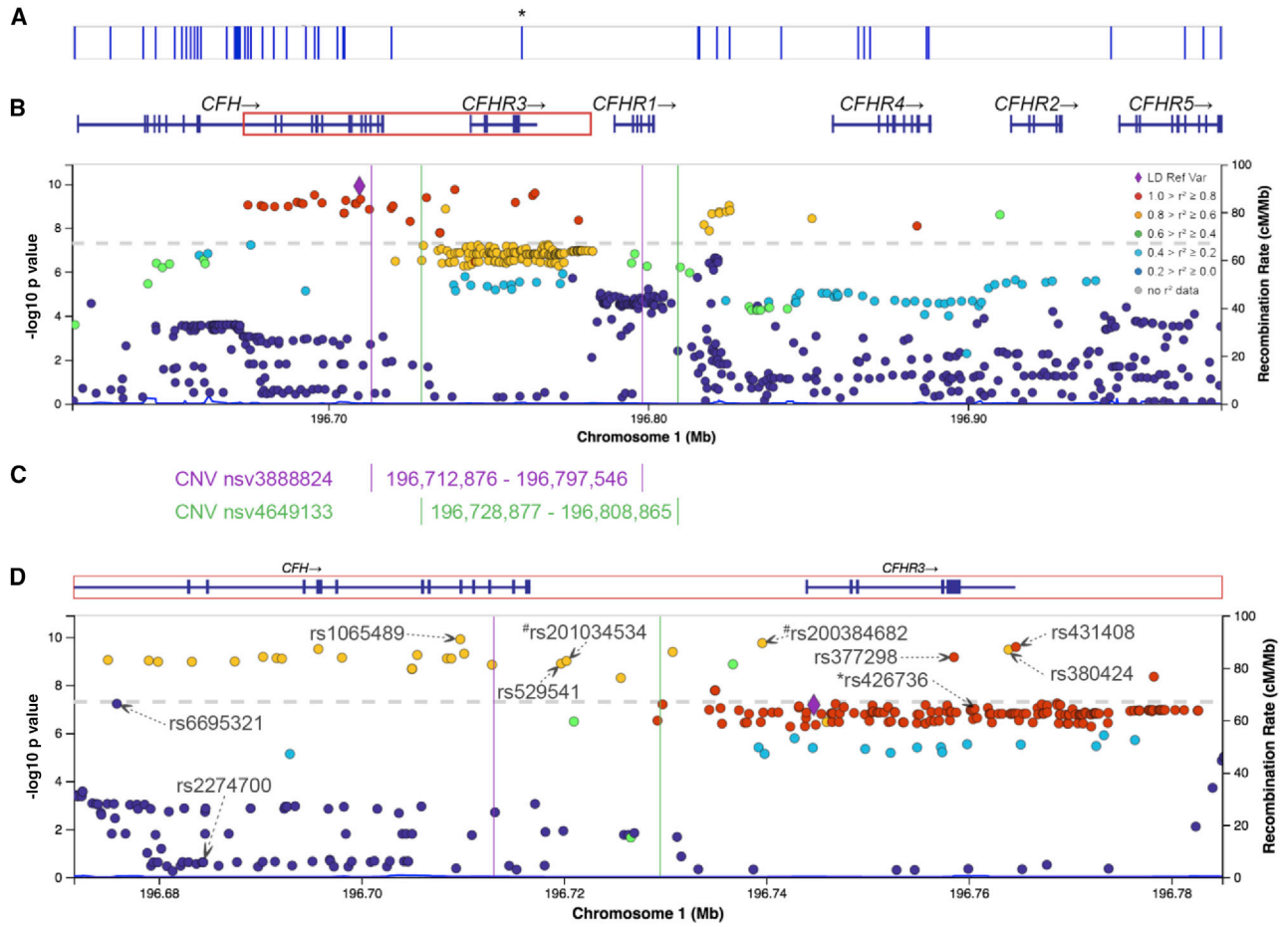

Figure 3. Fine mapping of the *CFH-CFHR* locus by GWAS

(A) Known variants reported in the NHGRI-EBI catalog of human genome-wide association studies. An asterisk represents the location of the rs426736 SNP within the CNVs and annotated as associated with MD.[10]

(B) The plot represents the genes located in the captured region (ranging from *CFH* to *CFHR5*) of the sequencing approach and shows association results of all variants (SNPs and InDels arranged according to their GRCh37/hg19 build chromosomal position on the x axis) from GWAS meta-analysis with the lead SNP, rs1065489, set as a reference variant (purple diamond). The color intensity of each symbol reflects the extent of LD with the top GWAS SNP.

(C) dbVar (https://www.ncbi.nlm.nih.gov/dbvar/)-annotated common CNVs with partial (nsv3888824 results in a *CFH/CFHR1* hybrid gene) or complete (nsv4649133) deletion of *CFHR3* and *CFHR1*.

(D) Plot showing association results of all variants (SNPs and InDels arranged according to their GRCh37/hg19 build chromosomal position on the x axis) from a GWAS meta-analysis with the lead SNP, rs75703017, from stages 1+2 set as a reference variant (purple diamond) mapping to a smaller genetic area focused on the start of the CNVs. Variants, which were either previously reported[10,36] or notable findings from this study (stages 1–3) are annotated within the plot. #Annotated variants represent small InDels within the CNVs. Violet vertical and green lines represent the start of the CNVs nsv3888824 and nsv4649133, respectively.

(HepG2) and of a line originating from embryonic kidney (HEK293T). We compared cells containing an empty vector (pGL3-empty) and three constructs containing the following: rs75703017 major allele C (pGL3-C); rs75703017 minor allele A (pGL3-A); and rs75703017 minor allele A together with minor alleles of two SNPs in close proximity (A of rs446868 and C of rs385390, pGL3-AAC) (Figure S7A, Table S12). Differential expression of a test reporter was detected in HepG2 (pGL3-A vs. pGL3-empty; $p < 0.0001$, Figure 5A) whereas HEK293T showed no significant change in expression (Figure S7B), supporting the liver-specific activity of the regulatory region.

Genome editing of the *CFHR3* region via CRISPR/Cas9 confirms its regulatory role in FH expression

To confirm that the identified *CFHR3* region regulates FH expression, we undertook genome editing by using CRISPR/Cas technology (Figures 5B and 5C, and supplemental Information). This required a liver cell line that constitutively expressed FH and carried at least one copy of *CFHR3*. Because none of the tested cell lines complied with both requirements, we differentiated human embryonic stem cells (H1 cell line) to hepatocytes.[41] H1 cells do not express FH or FHR-3 and carry only one copy of *CFHR3*. Upon differentiation to hepatocytes (Figure S8), we detected FH expression (Figure 5C, Table S13) supporting

Table 2. p values and ORs of the top 20 variants from the GWAS meta-analysis and of the 11 SNPs from the sequencing and genotyping

Variant ID	BP	Variant	Alt	Ref	MAF	OR	p_{meta}	I^2	DR^2
rs1065489[a]	196,709,774	missense	T	G	0.17	0.69	1.25×10^{-10}	0.74	gt
rs200384682	196,739,608[b]	indel	CA	C	0.18	0.69	1.81×10^{-10}	0.72	0.90
rs431408	196,764,663[b]	intron	G	T	0.20	0.69	2.62×10^{-10}	0.61	0.91
rs3753396	196,695,742	synonymous	G	A	0.17	0.69	3.21×10^{-10}	0.75	gt
rs380424	196,763,939[b]	downstream	C	T	0.18	0.69	3.38×10^{-10}	0.70	0.97
rs72482676	196,730,755[b]	intergenic	C	T	0.16	0.68	4.21×10^{-10}	0.73	0.96
rs11582939[a]	196,710,157	intron	T	C	0.17	0.70	4.99×10^{-10}	0.72	gt
rs742855[a]	196,705,520	intron	C	T	0.17	0.70	5.66×10^{-10}	0.76	gt
rs141408533	196,690,281	intron	T	TA	0.17	0.70	6.77×10^{-10}	0.75	1.00
rs377298	196,758,541[b]	3′ UTR	C	A	0.19	0.70	6.98×10^{-10}	0.61	0.93
rs77302817	196,698,082	indel	C	CTCTG	0.17	0.70	7.32×10^{-10}	0.76	1.00
rs12402808	196,691,625	intron	A	C	0.17	0.70	7.65×10^{-10}	0.76	1.00
rs11799380	196,708,455	intron	G	A	0.17	0.70	7.91×10^{-10}	0.73	1.00
rs2336221	196,708,891	intron	T	G	0.17	0.70	7.91×10^{-10}	0.73	1.00
rs11801630	196,692,148	intron	T	C	0.17	0.70	8.03×10^{-10}	0.75	gt
rs1048663	196,674,982	intron	A	G	0.17	0.70	9.14×10^{-10}	0.75	1.00
rs74861068	196,825,380	intron	A	G	0.13	0.65	9.60×10^{-10}	0.36	0.99
rs74213209	196,679,010	intron	G	A	0.17	0.70	9.65×10^{-10}	0.75	1.00
rs201034534	196,720,267[b]	indel	A	AAAAC	0.17	0.70	1.00×10^{-9}	0.74	0.99
rs10489456[a]	196,687,515	intron	A	G	0.17	0.70	1.05×10^{-9}	0.73	1.00
rs12409571	196,768,726[b]	intergenic	G	A	0.20	0.73	5.80×10^{-8}	0.57	0.87
rs116249058	196,767,218[b]	downstream	G	A	0.20	0.74	6.37×10^{-8}	0.53	0.87
rs75703017	196,744,699[b]	intron	A	C	0.20	0.74	6.80×10^{-8}	0.56	0.88
rs387107	196,757,881[b]	missense	T	G	0.21	0.74	7.19×10^{-8}	0.51	0.87
rs11807997	196,743,213[b]	upstream	G	A	0.20	0.74	8.68×10^{-8}	0.56	0.87
rs401188	196,757,083[b]	intron	T	C	0.21	0.74	1.30×10^{-7}	0.50	0.87
rs12408446	196,741,197[b]	upstream	A	G	0.21	0.74	1.38×10^{-7}	0.53	0.88
rs620015	196,748,676[b]	intron	G	A	0.21	0.74	1.47×10^{-7}	0.51	0.87
rs376841	196,746,600[b]	intron	C	T	0.21	0.75	1.53×10^{-7}	0.51	0.87
rs385390	196,743,927[b]	5′ UTR	C	A	0.21	0.75	2.36×10^{-7}	0.50	0.87
rs1329423	196,646,387	exon	C	T	0.26	0.79	4.09×10^{-7}	0.71	0.99

BP = base position (GRCh37/hg19); MAF = minor-allele frequency; OR = odds ratio (estimated from LMM beta effects according to https://shiny.cnsgenomics.com/LMOR/); DR^2 = mean dosage R-squared from the three single cohorts. gt = genotyped, no DR^2 score. SNPs from the sequencing and genotyping are indicated in italics.
[a]Previously reported as associated with MD susceptibility.
[b]Within a CNV (nsv3888824, nsv4649133).

the liver-specific expression reported previously.[40] Deletion of a 2.8 kb region (chr1: 196,743,825–196,746,668) within *CFHR3* containing rs75703017 via CRISPR/Cas9 in H1 cells (Figure 5B), followed by differentiation to hepatocytes, revealed enhanced FH expression, confirming the regulatory function of this region (Figure 5C). This finding is consistent with our t-test analysis (Table S7) of rs75703017 genotypes showing significant differential FH expression between deletion/major allele C (DC) and homozygous deletion (DD) genotypes ($p = 6.8 \times 10^{-3}$) and is further supported by Hi-C sequencing data, a strategy by which one can study three-dimensional architecture of the genome by coupling proximity-based ligation with massive parallel sequencing and that allows identification of long-range genomic interactions.[42] In two cell lines a long-range interaction could be observed between *CFH* and the association interval in *CFHR3* (Figure S9). Moreover, these results were concordant with *in vivo* data of individuals who were homozygous for the

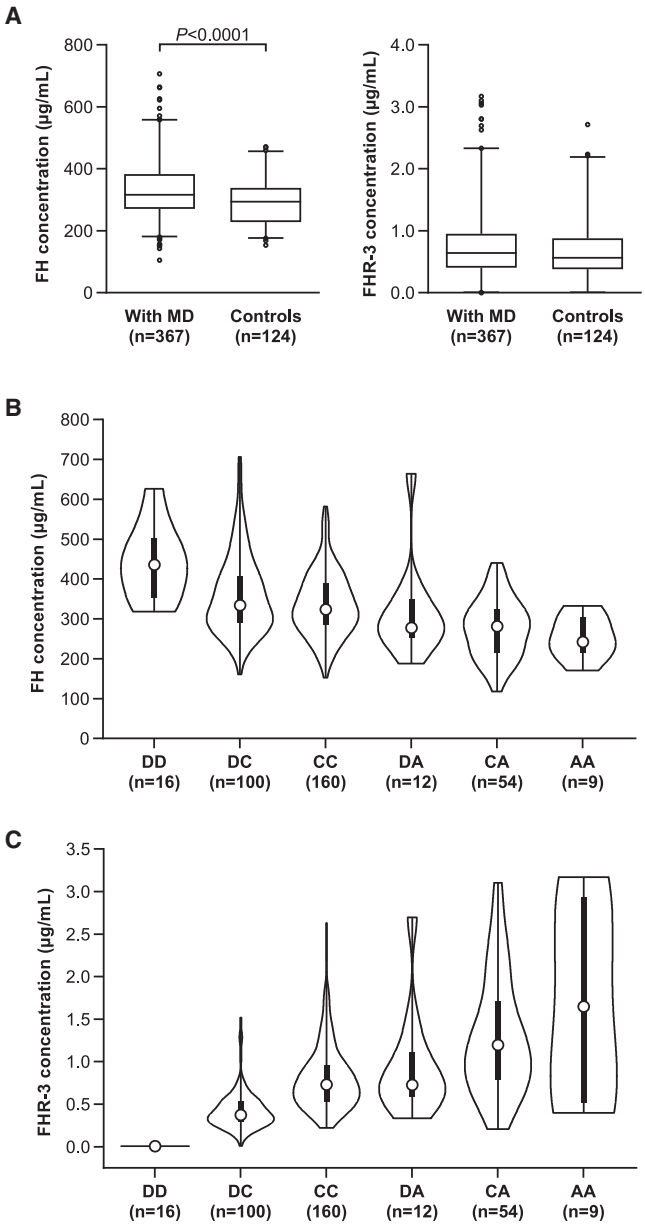

Figure 4. FH and FHR-3 concentrations in MD survivors

(A) Box plots with 95% range of FH serum concentrations (left panel), determined by ELISA. FH serum concentrations are increased ($p < 0.0001$, Mann-Whitney test) in MD survivors ($n = 367$) compared to healthy controls ($n = 124$), whereas FHR-3 serum concentrations are not significantly different between the two groups.

(B) Violin plotsof FH serum concentrations delineated by genotype for the SNP (rs75703017) most associated with FH concentrations; $p = 1.41 \times 10^{-11}$.

(C) Violin plot of FHR-3 serum concentrations delineated by genotype for the SNP (rs75703017), p value $< 2 \times 10^{-16}$.

For both (B) and (C), the x and y axes indicate genotypes and protein concentration (µg/mL), repsectively, with D = *CFHR3/CFHR1* deletion, A = minor allele, and C = major allele for rs75703017. The white dots indicate median concentrations, the thick black bars indicate the interquartile range, and the thin black bars represent total range. p values were estimated by ANCOVA.

CFHR3/CFHR1 deletion and who showed increased FH concentrations (Figure 4B).

Discussion

Genetic variants within *CFH* and the *CFHR* genes have been associated with genetic susceptibility to a range of human diseases.[17–21,43] Concordant with our work, deletion of *CFHR3-CFHR1* has been reported to alter FH concentrations in serum and modify genetic susceptibility to disease,[17,43,44] suggesting that a regulatory region controlling FH concentrations might exist at this locus.[17,43] Identification of the causal variants underlying these associations has been difficult because of the complexity of the region; CNVs and sequence homology hamper genotyping and sequencing efforts. Thus, previous reports relied on surrogate markers to identify the deletion. Our strategy here allowed us to type the CNV and polymorphisms in the *CFH-CFHR* region, to narrow the regulatory element to a short sequence in intron 1 of *CFHR3*, and to identify the complex interplay of six possible genotypes at one SNP locus, including the lead SNP and copy-number variant, with FH serum concentrations. Recent development of specific monoclonal antibodies for FH and FH-related proteins[33] allowed for an accurate detection of serum concentrations of FH and FHR-3.

We have fine mapped the complex *CFH-CFHR* region in individuals of European ancestry with MD and found that susceptibility and resistance to the disease is associated with a single SNP locus within intron 1 of *CFHR3*. This locus is affected by a well-known copy-number variant. Furthermore, by accounting for the protective effect of the minor allele (A) and the risk effect of the wild-type allele (C), we now demonstrate that the *CFHR3* deletion does associate, although to a lesser extent than the identified SNP, with increased susceptibility for MD. Previous studies[10,35] have missed this effect because their deletion analysis has combined the protective and risk alleles. Interestingly, the intronic lead SNP in *CFHR3*, rs75703017 ($p = 1.1 \times 10^{-16}$, OR = 0.63, 95% CI 0.55–0.71) lies in a liver-specific regulatory region that has been shown to loop and interact with *CFH* at the genomic level. This interaction seems to regulate *CFH* transcription activity. Protective homozygous rs75703017 A allele *CFHR3* genotypes were associated with low FH serum concentrations ($p = 1.41 \times 10^{-11}$), the homozygous rs75703017C allele genotype had higher FH serum concentrations. In our analyses, deletion of this region through genome editing in human embryonic stem cells differentiated to hepatocytes also showed a substantial increase (p value < 0.05) of *CFH* transcript concentrations and expression of FH protein.

We showed that individuals surviving MD had higher serum concentrations of FH than controls and that low concentrations of FH were protective for MD. This is concordant with our previous report showing that addition of excess FH to blood increases the survival of *N. meningitidis*.[45] Our data demonstrate that FH is a critical

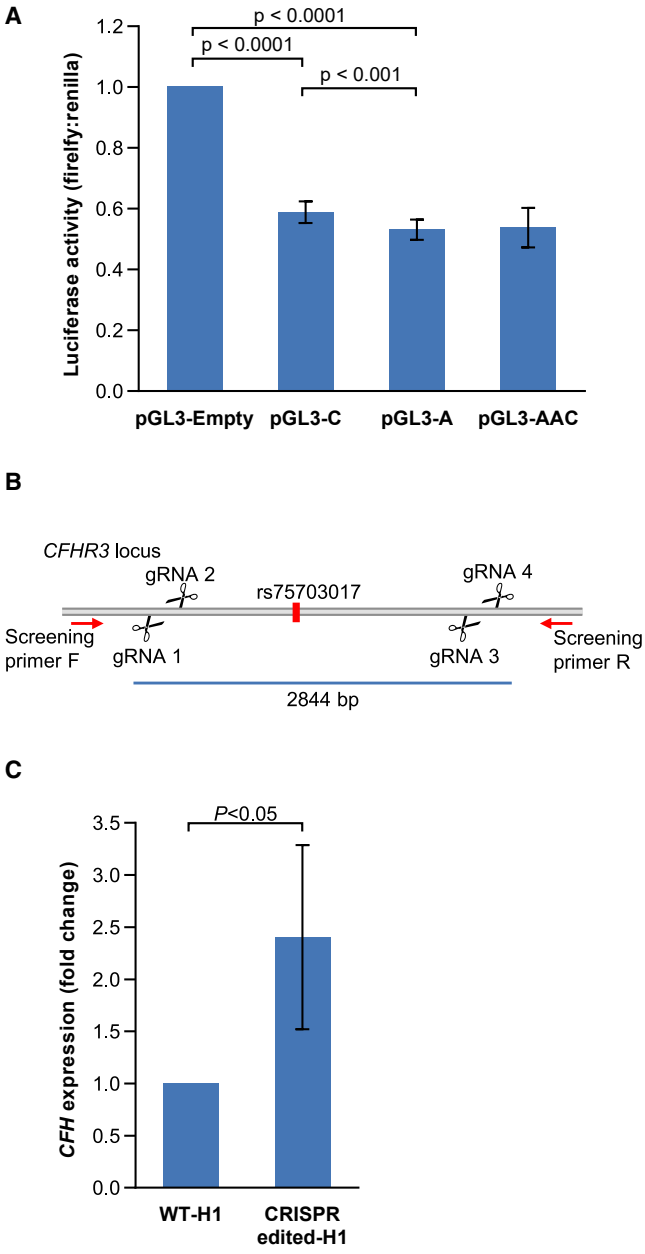

Figure 5. Functional validation of the top associated variant

(A) Effect of 2.8 kb regulatory sequence and the lead SNP, rs75703017, on reporter (firefly luciferase) activity in the HepG2 human liver cell line. pGL3-empty is an empty construct only containing a promoter, whereas pGL3-C contains the 2.8 kb regulatory sequence with major allele C at rs75703017, pGL3-A contains minor allele A at rs75703017, and pGL3-AAC contains minor allele A at rs75703017 and minor allele C at rs446868 and rs385390. Firefly luciferase concentrations were normalized to renilla luciferase activity for each sample, and all values were plotted relative to the pGL3-empty construct. The graph is representative of six independent experiments, and error bars represent means with standard deviation. Level of significance, calculated by t test, is indicated.

(B) Schematic depiction of CRISPR/Cas9 targeting of the *CFHR3* liver-specific regulatory region comprising 2,844 base pairs (chr1: 196,743,825–196,746,668). Excision sites of each guide RNA, located around the SNP of interest (rs75703017), are indicated by scissors. The position of screening primers designed for selection of positive clones with excision of the targeted region are indicated by red arrows.

(C) n-fold change, relative to the wild type, of *CFH* transcript expression levels of CRISPR-edited *CFHR3* (CRISPR-edited H1; genotype DD) carrying one copy of *CFHR3* with allele C (WT-H1; genotype DC) in liver-differentiated H1 human embryonic stem cells. Expression was measured by qRT-PCR. The graph represents three independent experiments with two biological replicates (different sets of gRNA were used for targeting; KO1 WT-Cas9 gRNA 1 and 3 and KO2 nickase-Cas9 gRNA 1, 2, 3, and 4; see Table S2) and one technical replicate of KO1. Error bars represent means with standard deviation. Level of significance, calculated by t test, is indicated. (D = *CFHR3*/*CFHR1* deletion, and C = major allele rs75703017).

complement regulatory protein associated with MD susceptibility and that its serum concentrations are controlled through a cis-regulatory element in intron 1 of *CFHR3*, independent of FHR-3 concentrations. Whereas previous studies have suggested that competition between FHR-3 and FH for the fHbp on the surface of *N. meningitidis* could be the mechanism controlling susceptibility to MD,[46] we suggest that serum concentrations of FHR-3 are too low to affect binding of the (on average) 132-fold more abundant FH to fHbp.[33] Our genetic analysis confirms this assumption. In fact, our data indicate that the effect on MD susceptibility is predominantly defined by regulation of FH concentrations in serum by genetic variation in *CFHR3*, irrespective of serum FHR-3 concentrations. A schematic explanation of the inhibition of meningococcal bactericidal activity of complement in human blood by FH and its regulation by genetic variation in *CFHR3* is shown in Figure 6. Importantly, our strongest genetic association is between low concentrations of serum FH and protection from disease, whereas high protein concentrations were less strongly associated with susceptibility. This suggests that *N. meningitidis* is able to harvest sufficient FH to prevent complement activity (thus ensuring serum survival) in most individuals and that high serum concentrations of FH only offer marginal additional bacterial protection as compared to average concentrations.

Our findings show that serum concentrations of FH are genetically regulated by a locus within *CFHR3*. Complement activation is an important immune protection mechanism against infections, but uncontrolled or excessive complement activation is potentially damaging to host cells and tissues. FH is a major regulator of complement-mediated damage to host cells[47] as highlighted by the severe diseases associated with inadequate concentration or function of FH; such diseases include TTP/aHUS,[20,37] glomerulonephritis,[18] other inflammatory diseases,[19] and AMD.[21] Next to *N. meningitidis*, many other pathogens (see also Moore et al.[27]), including *Streptococcus pneumoniae*,[48] group A streptococcus,[49] *Borrelia burgdorferi*,[50] and *Plasmodium falciparum*[51] possess FH-binding proteins and might use FH to evade complement-mediated killing. The genomic regulation of serum FH concentration that we have identified through genetic variation in *CFHR3* may thus be relevant to many other infectious and inflammatory diseases.

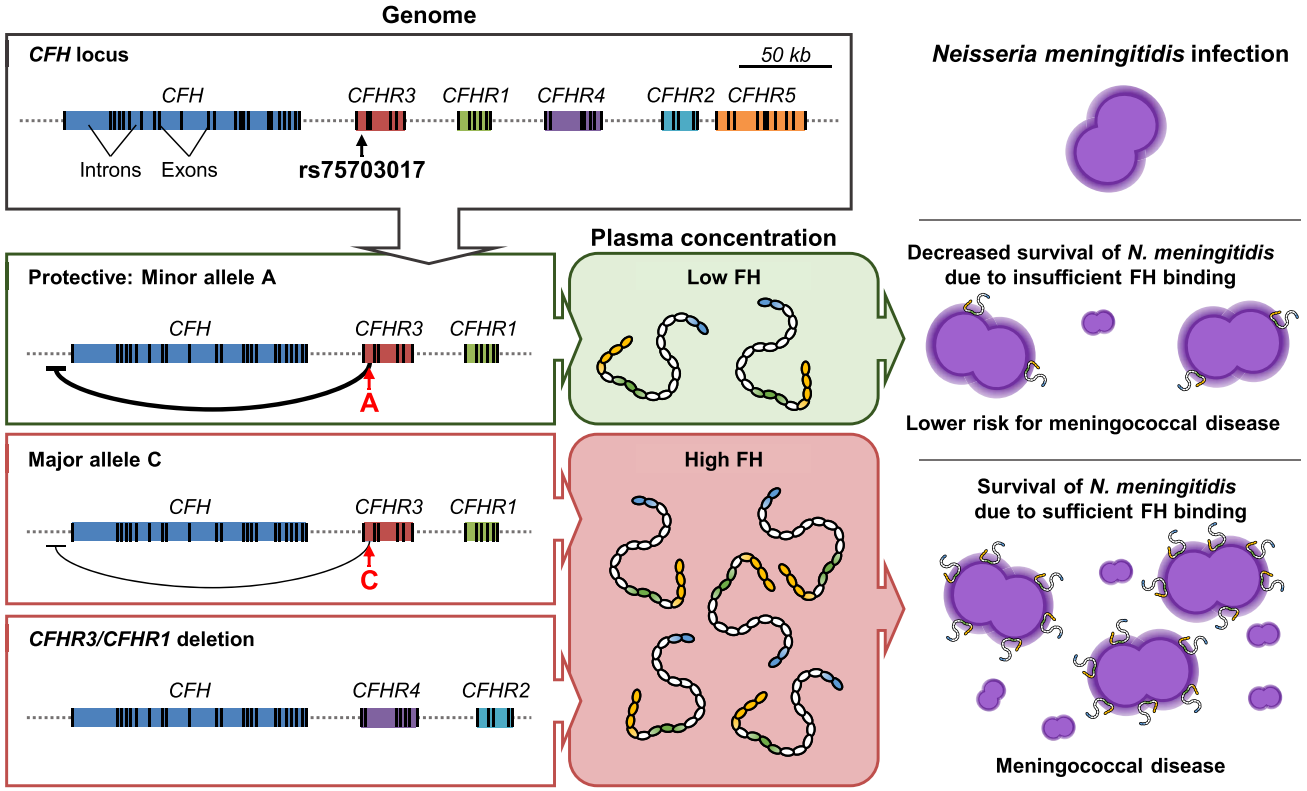

Figure 6. Schematic model of the effect of *CFHR3/CFHR1* deletion and SNP (rs75703017) on FH concentrations, interactions with *N. meningitidis*, and susceptibility to MD

The schematic diagram shows the structure of the gene region containing *CFH* and five *CFHR* genes. Carriers of the minor allele, A, on rs75703017 show the lowest FH concentrations. Increased concentrations of FH are found with the major allele, C, on rs7570317, whereas deletion of *CFHR3/CFHR1* is associated with the highest concentrations of FH. Susceptibility to MD is driven by FH serum availability, which increases binding to the meningococcal surface protein fHbp. This binding results in FH's impairing complement-mediated killing and allowing survival and growth of *N. meningitidis* in blood.

Data and code availability

Summary statistics of the genotyped analysis generated during this study are available at LocusZoom (https://my.locuszoom.org/gwas/552110/) and FUMA (https://fuma.ctglab.nl/browse/469). Other datasets supporting the current study have not been deposited in a public repository but are available from the corresponding authors upon reasonable request.

Supplemental information

Supplemental information can be found online at https://doi.org/10.1016/j.ajhg.2022.08.001.

Acknowledgments

We would like to thank all individuals who participated in this study. All samples have been collected under country-specific institutional review boards (UK EC3263; Netherlands: 37986.091.11/RvB12.51320; Austria: 24-116 ex 11/12; Spain: 2011/298; Swiss: Cantonal Ethics Committee, Inselspital, University of Bern, no. KEK- 029/11). This work has been partially supported by the European Seventh Framework Programme for Research and Technological Development (FP7) under EUCLIDS Grant Agreement n°. 279185, and by funding from the Agency for Science, Technology, and Research of Singapore (A*STAR). Additional funding supporting the establishment of the MD cohorts used in this study are kindly acknowledged and listed in the supplemental information.

Declaration of interests

R.B.P., M.C.B., D.W., and T.W.K. are co-inventors of patents or patent applications describing FH potentiating antibodies and uses thereof. A.J.P. is chair of the UK Department of Health and Social Care's Joint Committee on Vaccination and Immunisation. F.M.-T. has received honoraria from GSK group of companies, Pfizer Inc, Sanofi Pasteur, MSD, Seqirus, Biofabri, and Janssen for taking part in advisory boards and expert meetings and for acting as a speaker in congresses outside the scope of the submitted work. F.M.-T. has also acted as principal investigator in randomized controlled trials of the above-mentioned companies as well as Ablynx, Gilead, Regeneron, Roche, Abbott, Novavax, and MedImmune, with honoraria paid to his institution. All other authors declare no relevant competing interest related to the contents of this manuscript.

Received: April 9, 2022
Accepted: July 31, 2022
Published: September 1, 2022

References

1. Borrow, R., Alarcón, P., Carlos, J., Caugant, D.A., Christensen, H., Debbag, R., De Wals, P., Echániz-Aviles, G., Findlow, J., Head, C., et al. (2016). The Global Meningococcal Initiative: global epidemiology, the impact of vaccines on meningococcal disease and the importance of herd protection. Expert Rev. Vaccines *16*, 313–328.
2. Sridhar, S., Greenwood, B., Head, C., Plotkin, S.A., Sáfadi, M.A., Saha, S., Taha, M.-K., Tomori, O., and Gessner, B.D. (2015). Global incidence of serogroup B invasive meningococcal disease: a systematic review. Lancet Infect. Dis. *15*, 1334–1346.
3. Mustapha, M.M., Marsh, J.W., and Harrison, L.H. (2016). Global epidemiology of capsular group W meningococcal disease (1970-2015): Multifocal emergence and persistence of hypervirulent sequence type (ST)-11 clonal complex. Vaccine *34*, 1515–1523.
4. Xie, O., Pollard, A.J., Mueller, J.E., and Norheim, G. (2013). Emergence of serogroup X meningococcal disease in Africa: need for a vaccine. Vaccine *31*, 2852–2861.
5. Chow, J., Uadiale, K., Bestman, A., Kamau, C., Caugant, D.A., Shehu, A., and Greig, J. (2016). Invasive meningococcal meningitis serogroup C outbreak in Northwest Nigeria, 2015 – Third consecutive outbreak of a new strain. PLoS Curr. *8*. https://doi.org/10.1371/currents.outbreaks.06d10b6b4e690917d8b0a04268906143.
6. Campbell, H., Parikh, S.R., Borrow, R., Kaczmarski, E., Ramsay, M.E., and Ladhani, S.N. (2016). Presentation with gastrointestinal symptoms and high case fatality associated with group W meningococcal disease (MenW) in teenagers, England, July 2015 to January 2016. Euro Surveill. *21*. https://doi.org/10.2807/1560-7917.ES.2016.21.12.30175.
7. Bårnes, G.K., Kristiansen, P.A., Beyene, D., Workalemahu, B., Fissiha, P., Merdekios, B., Bohlin, J., Préziosi, M.P., Aseffa, A., and Caugant, D.A. (2016). Prevalence and epidemiology of meningococcal carriage in Southern Ethiopia prior to implementation of MenAfriVac, a conjugate vaccine. BMC Infect. Dis. *16*, 639.
8. Mbaeyi, S., Pondo, T., Blain, A., Yankey, D., Potts, C., Cohn, A., Hariri, S., Shang, N., and MacNeil, J.R. (2020). Incidence of meningococcal disease before and after implementation of quadrivalent meningococcal conjugate vaccine in the United States. JAMA Pediatr. *174*, 843–851.
9. Haralambous, E., Weiss, H.A., Radalowicz, A., Hibberd, M.L., Booy, R., and Levin, M. (2003). Sibling familial risk ratio of meningococcal disease in UK Caucasians. Epidemiol. Infect. *130*, 413–418.
10. Davila, S., Wright, V.J., Khor, C.C., Sim, K.S., Binder, A., Breunis, W.B., Inwald, D., Nadel, S., Betts, H., Carrol, E.D., et al. (2010). Genome-wide association study identifies variants in the CFH region associated with host susceptibility to meningococcal disease. Nat. Genet. *42*, 772–776.
11. Martinón-Torres, F., Png, E., Khor, C.C., Davila, S., Wright, V.J., Sim, K.S., Vega, A., Fachal, L., Inwald, D., Nadel, S., et al. (2016). Natural resistance to meningococcal disease related to CFH loci: Meta-analysis of genome-wide association studies. Sci. Rep. *6*, 35842.
12. Sjöholm, A.G., Jönsson, G., Braconier, J.H., Sturfelt, G., and Truedsson, L. (2006). Complement deficiency and disease: an update. Mol. Immunol. *43*, 78–85.
13. Fijen, C.A., Kuijper, E.J., te Bulte, M.T., Daha, M.R., and Dankert, J. (1999). Assessment of complement deficiency in patients with meningococcal disease in the Netherlands. Clin. Infect. Dis. *28*, 98–105.
14. Józsi, M., and Zipfel, P.F. (2008). Factor H family proteins and human diseases. Trends Immunol. *29*, 380–387.
15. Blaum, B.S. (2017). The lectin self of complement factor H. Curr. Opin. Struct. Biol. *44*, 111–118.
16. Parente, R., Clark, S.J., Inforzato, A., and Day, A.J. (2017). Complement factor H in host defense and immune evasion. Cell. Mol. Life Sci. *74*, 1605–1624.
17. Zhao, J., Wu, H., Khosravi, M., Cui, H., Qian, X., Kelly, J.A., Kaufman, K.M., Langefeld, C.D., Williams, A.H., Comeau, M.E., et al. (2011). Association of genetic variants in complement factor H and factor H-related genes with systemic lupus erythematosus susceptibility. PLoS Genet. *7*, e1002079.
18. Abrera-Abeleda, M.A., Nishimura, C., Smith, J.L.H., Sethi, S., McRae, J.L., Murphy, B.F., Silvestri, G., Skerka, C., Józsi, M., Zipfel, P.F., et al. (2006). Variations in the complement regulatory genes factor H (CFH) and factor H related 5 (CFHR5) are associated with membranoproliferative glomerulonephritis type II (dense deposit disease). J. Med. Genet. *43*, 582–589.
19. Kiryluk, K., Li, Y., Scolari, F., Sanna-Cherchi, S., Choi, M., Verbitsky, M., Fasel, D., Lata, S., Prakash, S., Shapiro, S., et al. (2014). Discovery of new risk loci for IgA nephropathy implicates genes involved in immunity against intestinal pathogens. Nat. Genet. *46*, 1187–1196.
20. Pickering, M.C., de Jorge, E.G., Martinez-Barricarte, R., Recalde, S., Garcia-Layana, A., Rose, K.L., Moss, J., Walport, M.J., Cook, H.T., de Córdoba, S.R., and Botto, M. (2007). Spontaneous hemolytic uremic syndrome triggered by complement factor H lacking surface recognition domains. J. Exp. Med. *204*, 1249–1256.
21. Hughes, A.E., Orr, N., Esfandiary, H., Diaz-Torres, M., Goodship, T., and Chakravarthy, U. (2006). A common CFH haplotype, with deletion of CFHR1 and CFHR3, is associated with lower risk of age-related macular degeneration. Nat. Genet. *38*, 1173–1177.
22. Cheng, C.Y., Yamashiro, K., Jia Chen, L., Ahn, J., Huang, L., Huang, L., Cheung, C.M.G., Miyake, M., Cackett, P.D., Yeo, I.Y., et al. (2015). New loci and coding variants confer risk for age-related macular degeneration in East Asians. Nat. Commun. *6*, 6817.
23. Lewis, L.A., Ngampasutadol, J., Wallace, R., Reid, J.E.A., Vogel, U., and Ram, S. (2010). The meningococcal vaccine candidate neisserial surface protein a (NspA) binds to factor H and enhances meningococcal resistance to complement. PLoS Pathog. *6*, e1001027.
24. Lewis, L.A., Vu, D.M., Vasudhev, S., Shaughnessy, J., Granoff, D.M., and Ram, S. (2013). Factor h-dependent alternative pathway inhibition mediated by porin B contributes to virulence of Neisseria meningitidis. mBio *4*, 1–9.
25. Giuntini, S., Pajon, R., Ram, S., and Granoff, D.M. (2015). Binding of Complement Factor H to PorB3 and NspA Enhances Resistance of Neisseria meningitidis to Anti-Factor H Binding Protein Bactericidal Activity. Infect. Immun. *83*, 1536–1545.
26. Schneider, M.C., Prosser, B.E., Caesar, J.J.E., Kugelberg, E., Li, S., Zhang, Q., Quoraishi, S., Lovett, J.E., Deane, J.E., Sim, R.B., et al. (2009). Neisseria meningitidis recruits factor H using protein mimicry of host carbohydrates. Nature *458*, 890–893.
27. Moore, S.R., Menon, S.S., Cortes, C., and Ferreira, V.P. (2021). Hijacking Factor H for Complement Immune Evasion. Front. Immunol. *12*, 602277–602323.

28. Agyeman, P.K.A., Schlapbach, L.J., Giannoni, E., Stocker, M., Posfay-Barbe, K.M., Heininger, U., Schindler, M., Korten, I., Konetzny, G., Niederer-Loher, A., et al. (2017). Epidemiology of blood culture-proven bacterial sepsis in children in Switzerland: a population-based cohort study. Lancet. Child Adolesc. Health *1*, 124–133.
29. Geishofer, G., Binder, A., Müller, M., Zöhrer, B., Resch, B., Müller, W., Faber, J., Finn, A., Endler, G., Mannhalter, C., et al. (2005). 4G/5G promoter polymorphism in the plasminogen-activator-inhibitor-1 gene in children with systemic meningococcaemia. Eur. J. Pediatr. *164*, 486–490.
30. Browning, B.L., Zhou, Y., and Browning, S.R. (2018). A One-Penny Imputed Genome from Next-Generation Reference Panels. Am. J. Hum. Genet. *103*, 338–348.
31. Zhou, X., and Stephens, M. (2012). Genome-wide efficient mixed-model analysis for association studies. Nat. Genet. *44*, 821–824.
32. Mägi, R., and Morris, A.P. (2010). GWAMA: software for genome-wide association meta-analysis. BMC Bioinf. *11*, 1–6.
33. Pouw, R.B., Brouwer, M.C., Geissler, J., van Herpen, L.V., Zeerleder, S.S., Wuillemin, W.A., Wouters, D., and Kuijpers, T.W. (2016). Complement factor H-related protein 3 serum levels are low compared to factor H and mainly determined by gene copy number variation in CFHR3. PLoS One *11*, e0152164.
34. Ang, L.T., Tan, A.K.Y., Autio, M.I., Goh, S.H., Choo, S.H., Lee, K.L., Tan, J., Pan, B., Lee, J.J.H., Lum, J.J., et al. (2018). A roadmap for human liver differentiation from pluripotent stem cells. Cell Rep. *22*, 2190–2205.
35. Bradley, D.T., Bourke, T.W., Fairley, D.J., Borrow, R., Shields, M.D., Zipfel, P.F., and Hughes, A.E. (2015). Susceptibility to invasive meningococcal disease: Polymorphism of complement system genes and Neisseria meningitidis factor H binding protein. PLoS One *10*, e0120757.
36. Sun, B.B., Maranville, J.C., Peters, J.E., Stacey, D., Staley, J.R., Blackshaw, J., Burgess, S., Jiang, T., Paige, E., Surendran, P., et al. (2018). Genomic atlas of the human plasma proteome. Nature *558*, 73–79.
37. Zipfel, P.F., Edey, M., Heinen, S., Józsi, M., Richter, H., Misselwitz, J., Hoppe, B., Routledge, D., Strain, L., Hughes, A.E., et al. (2007). Deletion of complement factor H-related genes CFHR1 and CFHR3 is associated with atypical hemolytic uremic syndrome. PLoS Genet. *3*, e41.
38. Bellos, E., Kumar, V., Lin, C., Maggi, J., Phua, Z.Y., Cheng, C.Y., Cheung, C.M.G., Hibberd, M.L., Wong, T.Y., Coin, L.J.M., and Davila, S. (2014). cnvCapSeq: detecting copy number variation in long-range targeted resequencing data. Nucleic Acids Res. *42*, e158.
39. Ward, L.D., and Kellis, M. (2012). HaploReg: A resource for exploring chromatin states, conservation, and regulatory motif alterations within sets of genetically linked variants. Nucleic Acids Res. *40*, D930–D934.
40. Kundaje, A., Meuleman, W., Ernst, J., Bilenky, M., Yen, A., Heravi-Moussavi, A., Kheradpour, P., Zhang, Z., Wang, J., Ziller, M.J., et al. (2015). Integrative analysis of 111 reference human epigenomes. Nature *518*, 317–330.
41. Loh, K.M., Ang, L.T., Zhang, J., Kumar, V., Ang, J., Auyeong, J.Q., Lee, K.L., Choo, S.H., Lim, C.Y.Y., Nichane, M., et al. (2014). Efficient endoderm induction from human pluripotent stem cells by logically directing signals controlling lineage bifurcations. Cell Stem Cell *14*, 237–252.
42. van de Werken, H.J.G., Landan, G., Holwerda, S.J.B., Hoichman, M., Klous, P., Chachik, R., Splinter, E., Valdes-Quezada, C., Öz, Y., Bouwman, B.A.M., et al. (2012). Robust 4C-seq data analysis to screen for regulatory DNA interactions. Nat. Methods *9*, 969–972.
43. Zhu, L., Zhai, Y.-L., Wang, F.-M., Hou, P., Lv, J.-C., Xu, D.-M., Shi, S.-F., Liu, L.-J., Yu, F., Zhao, M.-H., et al. (2014). Variants in complement factor H and complement factor H-related protein genes, CFHR3 and CFHR1, affect complement activation in IgA nephropathy. J. Am. Soc. Nephrol. *26*, 1195–1204.
44. Ansari, M., Mckeigue, P.M., Skerka, C., Hayward, C., Rudan, I., Vitart, V., Polasek, O., Armbrecht, A.-M., Yates, J.R.W., Vatavuk, Z., et al. (2013). Genetic influences on plasma CFH and CFHR1 concentrations and their role in susceptibility to age-related macular degeneration. Hum. Mol. Genet. *22*, 4857–4869.
45. Haralambous, E., Dolly, S.O., Hibberd, M.L., Litt, D.J., Udalova, I.A., O'dwyer, C., Langford, P.R., Simon Kroll, J., and Levin, M. (2006). Factor H, a regulator of complement activity, is a major determinant of meningococcal disease susceptibility in UK Caucasian patients. Scand. J. Infect. Dis. *38*, 764–771.
46. Caesar, J.J., Lavender, H., Ward, P.N., Exley, R.M., Eaton, J., Chittock, E., Malik, T.H., Goiecoechea De Jorge, E., Pickering, M.C., Tang, C.M., and Lea, S.M. (2014). Competition between antagonistic complement factors for a single protein on N. meningitidis rules disease susceptibility. Elife *3*, e04008.
47. Ferluga, J., Kouser, L., Murugaiah, V., Sim, R.B., and Kishore, U. (2017). Potential influences of complement factor H in autoimmune inflammatory and thrombotic disorders. Mol. Immunol. *84*, 84–106.
48. Janulczyk, R., Iannelli, F., Sjöholm, A.G., Pozzi, G., and Björck, L. (2000). Hic, a novel surface protein of Streptococcus pneumoniae that interferes with complement function. J. Biol. Chem. *275*, 37257–37263.
49. Haapasalo, K., Jarva, H., Siljander, T., Tewodros, W., Vuopio-Varkila, J., and Jokiranta, T.S. (2008). Complement factor H allotype 402H is associated with increased C3b opsonization and phagocytosis of Streptococcus pyogenes. Mol. Microbiol. *70*, 583–594.
50. Kraiczy, P., Skerka, C., Kirschfink, M., Brade, V., and Zipfel, P.F. (2001). Immune evasion of Borrelia burgdorferi by acquisition of human complement regulators FHL-1/reconectin and factor H. Eur. J. Immunol. *31*, 1674–1684.
51. Kennedy, A.T., Schmidt, C.Q., Thompson, J.K., Weiss, G.E., Taechalertpaisarn, T., Gilson, P.R., Barlow, P.N., Crabb, B.S., Cowman, A.F., and Tham, W.-H. (2016). Recruitment of factor H as a novel complement evasion strategy for blood-stage Plasmodium falciparum infection. J. Immunol. *196*, 1239–1248.

The American Journal of Human Genetics, Volume *109*

Supplemental information

Variation in *CFHR3* determines susceptibility to meningococcal disease by controlling factor H concentrations

Vikrant Kumar, Richard B. Pouw, Matias I. Autio, Manfred G. Sagmeister, Zai Yang Phua, Lisa Borghini, Victoria J. Wright, Clive Hoggart, Bangfen Pan, Antson Kiat Yee Tan, Alexander Binder, Mieke C. Brouwer, Ellie Pinnock, Ronald De Groot, Jan Hazelzet, Marieke Emonts, Michiel Van Der Flier, Karl Reiter, Markus M. Nöthen, Per Hoffmann, EUCLIDS consortium, Luregn J. Schlapbach, Evangelos Bellos, Suzanne Anderson, Fatou Secka, Federico Martinón-Torres, Antonio Salas, Colin Fink, Enitan D. Carrol, Andrew J. Pollard, Lachlan J. Coin, Werner Zenz, Diana Wouters, Lay Teng Ang, Martin L. Hibberd, Michael Levin, Taco W. Kuijpers, and Sonia Davila

Supplementary Appendix

Table of Contents

Supplementary Methods

Supplementary Methods

1 Study Sample Set

An overview about the cohorts and used methods can be found in Figure S1 and Table S1. Clinical details of the individuals with meningococcal disease (MD) and controls were described previously[1]. In brief meningococcal disease was diagnosed based on isolation of *N. meningitidis* from blood or CSF, or detection of meningococcal genome by PCR in children presenting with purpuric rash, meningitis or septic shock. Cases without microbiological confirmation were included if they presented with the characteristic picture of purpura fulminans, and other bacterial or viral causes of critical illness had been excluded. Samples for DNA extraction (EDTA blood) and plasma (recovered from EDTA Blood) and serum both at the time of admission and after recovery were stored at -80°C until used.

European Childhood Life threatening Infection study (EUCLIDS)

EUCLIDS is an EU FP7 funded study that prospectively recruited children with fever and signs of infection presenting to hospitals in nine EU countries. Full details of the study have been reported[2]. The study included individuals with blood culture-proven sepsis recruited in the Swiss Pediatric Sepsis Study[3]. Individuals were categorized as having definite bacterial infection if a causative organism was identified on blood, CSF, urine or other sterile site by either culture or molecular methods. Individuals were considered to have probable bacterial infection if they had shock, pneumonia, meningitis, osteomyelitis or severe focal infection, high white cell count or CRP, but no causative pathogens were identified. DNA from individuals with MD was isolated from blood and sent for genotyping on Illumina exome chip arrays at the Genome Institute of Singapore (GIS).

Ethics and Consent; Informed consent was obtained from parents or guardians. The study was approved by the research ethics bodies of each collaborating partner (UK EC3263; Netherlands: 37986.091.11 / RvB12.51320; Austria: 24-116 ex 11/12; Spain: 2011/298; Switzerland KEK-029/11). In addition to the local approvals for use of retrospective MD cohorts the EUCLIDS study was approved by each partner country research ethics bodies.

Central European Cohort (CEC) for genome-wide association study (GWAS)

Individuals with MD and blood donors from Central Europe were previously published[4] and additional individuals with MD and controls were recruited beyond the publication. DNA was isolated using standard procedures and genotyped on Illumina HumanOmni 1M Quad Microarray at the GIS. The final cohort consisted of 409 individuals with MD comprising individuals of Austrian, German, Swiss, Italian and Dutch ancestry. Controls consisted of 500 cord blood donors of healthy infants from Austria, 134 blood donors from Amsterdam and 1,242 German participants from the Heinz Nixdorf Recall study[5] which were randomly chosen from three German cities and genotyped on an Illumina HumanOmniExpress-12v1 Microarray.

2 Study Design

We followed a multiple-stage study design to conduct genetic association studies (Figure S1 and Table S1). First we deep-sequenced the *CFH-CFHR* region in 475 individuals comprising of 238 individuals with MD and 237 controls from a Central European cohort. Heterogeneity scores indicated that there was no significant population admixture between individuals with MD and controls. Replication analyses were carried out on 4,194 individuals which includes three cohorts from the UK (755 individuals with MD, 1,253 controls), Central Europe (279 individuals with MD, 395 controls) and Spain (488 individuals with MD, 1,024 controls) that have been previously described[1]. Later we performed genome-wide association studies (GWASs) in previously genotyped samples from three European cohorts followed by a meta-analysis including 1,246 individuals with MD and 7,197 controls. In addition, serum concentrations of FH and FHR-3 were measured in 308 UK and 59 Dutch survivors of MD (at least 6 months after the acute illness) and 124 Caucasian unrelated controls. Protein quantitative trait loci (pQTL) analysis was performed in 295 UK samples and replicated in a cohort of 56 Central European individuals. Finally, we performed functional analyses on different cell lines using Dual-Luciferase Assays and CRISPR/Cas9 technology.

3 Fine mapping by sequencing and variant calling (stage 1)

The *CFH* region spanning 359 kb in chr1 (chr1:196,620,000-196,979,000, GRCh37/hg19) consists of *CFH* and the *CFHR* genes which show high sequence identity and are a great challenge to sequence. With Nimblegen SeqCap EZ choice library we made probes to capture ~80% of the whole region and performed targeted resequencing (Figure S2a). Deep sequencing was carried out on Illumina HiSeq 2000 using 100bp paired-end read sequencing protocol. Image analysis and base calling was done by Illumina pipeline with default parameters. Sequence reads were mapped to the reference genome (GRCh37/hg19) using the ELAND module of CASAVA v1.8.2 program. Multi-mapped reads were not considered for further analysis and duplicate reads were identified by Picard (http://picard.sourceforge.net/) and removed. This was followed by local realignment and base quality score recalibration of the reads and finally variant calling by GATK 3.3. The mean depth of coverage for all samples was estimated to be ~227X ± 47, with ~95% of the region having 5X or more depth of coverage (Figure S2b).

Single Nucleotide polymorphisms (SNPs) were called for all Central European samples together using the Unified Genotyper module of GATK 3.3. To obtain high quality variants SNPs with i) a quality score < 50 or ii) QD < 2 or iii) FS > 60 or iv) MQ < 40 or v) haplotype score > 13 or vi) MQRankSum < -12.5 or vii) ReadPosRankSum < -8 were removed.

4 Validation by genotyping (stage 2)

The top 51 SNPs were selected for validation in three cohorts of European descent using a Sequenom Multiplex MassArray (San Diego, USA). Six SNPs failed to be designed due to the mentioned complexity of the region.

We also genotyped these SNPs on 295 UK individuals and 56 Central Europeans (mentioned above) included on a quantitative trait analysis.

5 CNV calling and validation

A novel method, cnvCapSeq[6] that can detect copy number variation (CNV) in long-range targeted resequencing data, was applied to call CNVs in our sequencing effort. CNV results were validated using quantitative PCR (qPCR) on a randomly chosen subset of samples (n=67), in triplicates. To confirm that the primers (Table S2 in the Supplementary Appendix) were targeting the intended region, we performed PCR and Sanger sequencing in one sample. As internal control a 5th set of primers for *PRKG1* (a house keeping gene) were designed. Following qPCR, copy number estimates were obtained using the ΔΔCt method of relative quantification.

In the second stage of CNV validation all three European cohorts were assessed by Taqman assays (1,463 controls and 1,302 cases). To call CNVs we used CopyCaller v2.0 program and a known reference with two copies. A subset of samples (~5%) was validated using qPCR. We also typed additional 295 UK samples using qPCR (described above) and 56 Central European samples using qPCR and Multiplex Ligation-dependent Probe Amplification (MLPA) (Table S10 in the Supplementary Appendix).

6 Genome-wide association studies (GWAS) and subsequent meta-analysis (stage 3)

The three cohorts from Central Europe (CEC), UK and Spain comprised of following number of samples: 409 individuals with MD and 1,876 controls in the CEC, 475 individuals with MD and 5,069 controls in the UK cohort and 422 individuals with MD and 910 controls in the Spanish cohort. Quality controls (QCs), filtering and associations were performed in all three cohorts separately to mitigate the effect of population stratification using, if not otherwise stated, PLINK v1.90b6.18 [7] and PLINK v2.00a2.3LM [7] according to the following scheme: i) merging of cases and controls; ii) pruning the dataset for common and independend SNPs with subsequent removal of samples with excessive heterozygosity (± 3 SD), sex mismatches, 1st degree related samples (identity by descent with PI_HAT ≥ 0.185) by removing one of a pair (either the less severe cases or controls with the lower genotyping call rate were dropped); iii) automatic removal of principal components (PCs) analysis-defined population outliers (>6x SD) based on the unrelated, cleaned and pruned dataset using the EIGENSOFT[8,9] package; iv) removal of samples and variants according to following filter criteria: MAF <1%, call rates (samples and variants) <95%, deviation from Hardy-Weinberg equilibrium (HWE) with a P-value of $<10^{-6}$ (in controls only) and ambiguous SNPs (C/G, A/T at a given locus)

identified with SNPflip v0.0.6 (https://github.com/biocore-ntnu/snpflip); v) investigation and correction of allele strand issues by flipping and swapping affected alleles was done with BCFtools v1.9 (https://github.com/samtools/bcftools) aligned to the 1,000 genomes project (1KGP) phase 3 genome assembly before haplotype estimation ("phasing") and imputation of missing genotypes with a subset (https://ega-archive.org/datasets/EGAD00001002729) of the Haplotype Reference Consortium (HRC) Release 1.1[10] containing 11,227 samples of European ancestry and the 1KGP[11] as references using Beagle 5.1[12,13]; vi) post-imputation QCs removed samples and variants (HRC with SNPs only; 1000 genomes including SNPs, small insertions and deletions) using the same thresholds mentioned above plus all imputed variants with a Dosage R-squared score ≤85% (DR2; estimated squared correlation between estimated REF dose [P(RA) + 2*P(RR)] and true REF dose); vii) extraction of allele dosages (continuous variable between 0 = homozygote for REF allele and 2 = homozygote for ALT allele) for each variant in every individual and data preparation for the association were done with BCFtools v1.9 and PLINK 2.00a; viii) associations on single cohorts were performed using an univariate linear mixed model (uLMM) algorithm implemented in GEMMA v0.98.1[14] using quantitative traits and including the first 2 PCs for the UK cohort and the first 4 PCs for the CEC and the Spanish cohort previously calculated on independent genotyped SNPs performed with the EIGENSOFT package ix) meta-analysis on summary statistics resulting from the GEMMA uLMM was performed with GWAMA[15] v2.2.2 having '--indel_alleles' and '--genomic_control' activated; x) visualisation of data (Manhattan-, QQ-, and PCA plots) was done with R statistical program v3.5.1[16] and the online tool LocusZoom (https://my.locuszoom.org/) was used for the regional association plots whereby linkage desiquillibrium (LD) was estimated based on the 1KGP EUR population according to the GRCh37/hg19 genome build coordinates. Post GWAS analysis using SNP2GENE and GENE2FUNC tools implemented in the online tool FUMA (https://fuma.ctglab.nl/) did not reveal any new insights for the *CFH/CFHR* gene region.

7 MLPA

The MLPA kit SALSA MLPA probemix P236-A3 ARMD mix-1 was used to genotype the *CFH-CFHR* gene region according to the manufacturer's instructions (MRC-Holland, Amsterdam, the Netherlands).

8 FH and FHR-3 ELISA

FH and FHR-3 levels in serum were determined by highly specific ELISA's previously described[17]. In short, FH was measured by ELISA using an in-house developed, highly specific mouse monoclonal antibody (mAb) directed against SCR domains 16/17 of FH (clone anti-FH.16, Sanquin Research, Amsterdam, The Netherlands), as the capture mAb and using polyclonal goat anti-human FH (Quidel, San Diego, CA, USA), which was HRP-conjugated, as the conjugate. For the specific detection of FHR-3, an in-house developed mAb directed against FHR-3 and FHR-4A was used as the capture antibody. A biotinylated mAb directed against FHR-3 and FH was used as conjugate.

FH and FHR-3 serum levels of all samples together with their genotypes are reported in Table S10 in the Supplementary Appendix.

9 Statistical analysis

We first carried out association testing using Fisher's exact test for rare SNPs and logistic regression analysis for common SNPs and CNV under an additive genetic model in the Central European sequenced samples (PLINK v1.07; http://pngu.mgh.harvard.edu/purcell/plink/). This was done after removing samples that were related (using genome wide SNP data available[1]) and showing the lack of population stratification (lambda=1). We also observed that the allele frequencies of the SNPs based on a cohort excluding the samples with CNV as similar to the cohort having samples with CNV, thus allowing us to consider all the samples for analysis. The P-values obtained from the Central European cohort were utilized as cut-offs to choose SNPs selected for replication. To mitigate the effect of population stratification, association of SNPs with MD was analyzed separately in all three replication cohorts under the additive model using logistic regression analysis and Fisher's exact test. Finally, meta-analysis both for SNPs and a CNV was performed by combining the summary statistics of stage 1 and 2 data in European populations using the Cochran-Mantel-Haenszel (CMH) test after testing for between-study heterogeneity with the Breslow-Day test. In addition, for CNV all the samples were combined and analyzed under genotypic and additive model after

removing samples carrying allele ‘C’. Regional plots of association were generated using LocusZoom with the GRCh37/hg19 genome build and LD pattern from 1,000 Genomes project EUR population. A forest plot was made using the metafor package in R. The meta-analysis P-value was estimated by Inverse-variance fixed-effect model.

We performed ANCOVA, with sex as a covariate, to estimate the overall difference in the protein levels across six genotype groups. To assess the difference of protein levels between two genotype groups we also performed a t-test (after adjusting for multiple comparisons tests using Holm’s method).

Genotype-phenotype correlation of SNPs in Europeans was analyzed for FH and FHR-3 protein level using linear regression analysis following the additive model. We combined UK and Central Europe samples QTL dataset to conduct fixed-effects meta-analysis after assessing the level of heterogeneity between both cohorts. Regional plots of QTL analysis were generated using LocusZoom using GRCh37/hg19 genome build and LD pattern from 1,000 Genomes project EUR population. To study the effect of SNPs on protein levels, we only considered samples without deletions and performed a QTL analysis.

10 Identification of Regulatory elements

Using haploreg v3[18], we annotated the liver specific regulatory element in the *CFH-CFHR* region. To further confirm it Road Map ChIP-seq data showing active promoter region predicted only in the E066 liver cell-line by H3K4me3 and H3K9ac (in duplicates) were analyzed (http://epigenomegateway.wustl.edu/browser/). To understand the plausible mechanism by which the regulator elements govern the gene expression of *CFH*, we analyzed UCSD Hi-C H1 and IMR90 data (http://epigenomegateway.wustl.edu/browser/) with 20 kilobases resolutions (in duplicates).

11 Luciferase assay

For plasmid construction (primers listed in Table S12 in the Supplementary Appendix), the putative 2.8 kb regulatory sequence was amplified from H1 hES genomic DNA for the major allele of rs75703017 (pGL3-

C) using luci 5' F and 3' R primers. Regulatory sequences containing the minor allele of rs75703017 (pGL3-A) and minor allele of rs75703017 and minor alleles of two close SNPs identified (A for rs446868 and C for rs385390) to rs75703017 (pGL3-AAC) were amplified from gBlocks designed with the specified SNPs and H1 gDNA (luci 5' F, 5' R, 3' F and 3' R primers). The amplified fragments were ligated to the SalI cut site of pGL3-Promoter (Promega, E1761) plasmid. We chose rs446868 and rs385390 to determine if we could observe additional regulatory effect or independent effect (if rs75703017 does not show any regulatory effect). These two SNPs were in perfect LD (based on 1000 genome data; http://archive.broadinstitute.org/mammals/haploreg/haploreg.php), most proximal (one upstream in the 5'-UTR region and one before that) with the lead SNP.

The luciferase assays were conducted with Dual-Glo® Luciferase Assay System (Promega, E2920) using the GloMax®-Multi+ Detection system according to manufacturer's instructions. The pGL3-Promoter constructs were transfected into HepG2 and HEK293T cells with Lipofectamine 3000 (ThermoFisher, L3000015), according to manufacturer's instructions. Briefly, 40,000 and 25,000 cells per well of HepG2 and HEK293T respectively were seeded in 96-well plates. After 24h the cells were transfected with 0.5 µL of lipofectamine and 100 ng of each pGL3-Promoter plasmid and 10 ng of pRL-SV40 (renilla) plasmid per well. Luciferase analysis was done 48h after transfection. At least three replicate wells were analysed for each test condition and the experiment was repeated three times (twice for HEK293).

Each experiment, measured in triplicates or more, was normalized by dividing the test reporter (Firefly luciferase) activity by the internal control reporter (Renilla luciferase) activity. The normalized values were then averaged. To compare the estimates between different experiments we further normalized fold-change between different construct/test groups by dividing the average value of a construct with the average value of another construct. To determine the significance of fold–change we calculated P-value using single sample t-test.

12 Human embryonic stem cells differentiation

Wild type and CRISPR/Cas targeted H1 hES cells were maintained on Geltrex coated plates (Thermo Fisher, A1413302) in mTeSR1 or TeSR E8 (Stemcell technologies, #05850 &#05940). Cells were differentiated to hepatocyte like cells over 18 days as previously described[19].).

13 Genome editing of differentiated hepatocytes by CRISPR/Cas9

Guide RNAs flanking the liver specific regulatory region were designed using the online CRISPR design tool at http://crispr.mit.edu/ and the gRNAs with the best available on target and off target scores were selected after *in vitro* testing (Table S3 in the Supplementary Appendix). The guide RNAs selected for targeting experiments were used with 2sg-SpCas92AClover and 4sg-nSpCas92AClover plasmids and electroporated into H1 hES cells with Amaxa 4D nucleofector (Lonza). Following the treatment cells were plated out for two days to recover. After this the cells underwent FACS for Clover+ cells to enrich for CRISPR/Cas targeted cells. Clover+ cells were seeded at a low density (500 -1,000 cells per one 6-well). After 2-3 weeks of culture single colonies were picked from the wells and expanded for screening and frozen for stock. Deletion of liver specific regulatory region was determined by PCR with primers spanning the targeted region (Table S13 in the Supplementary Appendix). Confirmed deletion clones and wild type controls were used in downstream analysis.

14 Construction of plasmids

Primers used for constructing the plasmids are listed in Table S12 in the Supplementary Appendix. All restriction enzymes were purchased from NEB, unless stated otherwise. PCR reactions were conducted using Q5® Hot Start High-Fidelity 2X Master Mix (NEB, M0494L) or Phusion High-Fidelity PCR Master Mix with HF Buffer (ThermoFisher Scientific, F531S). Ligations were conducted using isothermal assembly with NEBuilder® HiFi DNA Assembly Master Mix (NEB, E2621L) or In-Fusion® HD EcoDry™ Cloning Plus (Clontech, 638915). Primers and dsDNA fragments were ordered from IDT.

EF1a promoter was PCR amplified from N205 plasmid (Addgene plasmid # 44017), a gift from Jerry Crabtree[20], and Amp pUC fragment from pCMV-Bsd (Thermo, V51020). Plasmids pX330 and pX335

(Addgene plasmid # 42230 & # 42335), gifts from Feng Zhang[21], were digested with XbaI & AarI (Thermo, ER1582) and EF1a was ligated in. The modified plasmids were digested with SspI and XbaI and Amp pUC fragment ligated. DNA fragments encoding BsmBI, AarI and BspQI chimaeric gRNA cassettes were amplified from gBlocks and BbsI chimaeric gRNA cassette amplified from px335. The cassettes were subsequently ligated into XbaI site of the EF1a-SpCas9 & EF1a-nSpCas9 plasmids to make 2sg and 4sg plasmids respectively. The plasmids were digested with PmlI and EcoRI, Cas9 3' fragments were amplified from 2sg and 4sg plasmids and 2AClover fragment was amplified from a gBlock. The Cas9 3' fragments were respectively ligated together with the 2AClover fragment and the digested plasmids to make the final 2sg-SpCas92AClover and 4sg-nSpCas92AClover plasmids.

16 gRNA testing

The designed gRNAs were tested using a GFP reconstitution assay[22]. Briefly, the liver specific regulatory region was amplified from H1 gDNA and inserted into SalI cut site of pCAG-EGxxFP plasmid (Addgene plasmid # 50716), a gift from Masahito Ikawa. Designed gRNAs were cloned into the BbsI cut sites of px330 plasmid. The target plasmid and each of the tested gRNA plasmids were transfected into HEK293T cells at a 1:1 ratio using 5 μg Polyethylenimine per 1μg of DNA. The expression of GFP was observed after 48h and the most efficient gRNAs were selected for targeting of hES.

17 RT-qPCR

Total RNAs were extracted from undifferentiated and liver differentiated cells with the RNeasy kit (Qiagen) according to manufacturer's instruction. RNA integrity and quantity were checked by running the samples on a Bioanalyzer RNA 6000 Nano chip (Agilent). One microgram of total RNAs were used for reverse transcription using QuantiTect Reverse Transcription kit (Qiagen) followed by qPCR with LightCycler 480 SYBR Green I Master (Roche) according to the manufacturers' instructions. The following PCR program was used: 5 minutes at 95°C; 45x (10 seconds at 95°C, 1 minute at 65°C, 30 seconds at 72°C). The ΔΔCt method was applied to determine the fold change in expression of the genes of interest, by normalizing

with the housekeeping gene *GADPH*. Liver markers were tested on liver differentiated cells versus undifferentiated cells. *CFH* expression was investigated in *CFHR3*-deleted cells versus wild type. Sequences of the primers used for qPCR are shown in Table S13 in the Supplementary Appendix. To determine the significance of fold–change we calculated P-value using single sample t-test.

References

1. Davila S, Wright VJ, Khor CC, et al. Genome-wide association study identifies variants in the CFH region associated with host susceptibility to meningococcal disease. Nat Genet 2010;42(9):772–6.

2. Martinón-Torres F, Salas A, Rivero-Calle I, et al. Life-threatening infections in children in Europe (the EUCLIDS Project): a prospective cohort study. Lancet Child Adolesc Heal 2018;2(6):404–14.

3. Agyeman PKA, Schlapbach LJ, Giannoni E, et al. Epidemiology of blood culture-proven bacterial sepsis in children in Switzerland: a population-based cohort study. Lancet Child Adolesc Heal [Internet] 2017;1(2):124–33. Available from: http://dx.doi.org/10.1016/S2352-4642(17)30010-X

4. Geishofer G, Binder A, Müller M, et al. 4G/5G promoter polymorphism in the plasminogen-activator-inhibitor-1 gene in children with systemic meningococcaemia. Eur J Pediatr 2005;164(8):486–90.

5. Mahabadi AA, Möhlenkamp S, Moebus S, et al. The Heinz Nixdorf Recall Study and its potential impact on the adoption of atherosclerosis imaging in European primary prevention guidelines. Curr Atheroscler Rep 2011;13(5):367–72.

6. Bellos E, Kumar V, Lin C, et al. cnvCapSeq: detecting copy number variation in long-range targeted resequencing data. Nucleic Acids Res 2014;42(20):e158.

7. Chang CC, Chow CC, Tellier LCAM, Vattikuti S, Purcell SM, Lee JJ. Second-generation PLINK: Rising to the challenge of larger and richer datasets. Gigascience 2015;4(1):1–16.

8. Price AL, Patterson NJ, Plenge RM, Weinblatt ME, Shadick NA, Reich D. Principal components analysis corrects for stratification in genome-wide association studies. Nat Genet 2006;38(8):904–9.

9. Patterson N, Price AL, Reich D. Population structure and eigenanalysis. PLoS Genet 2006;2(12):2074–93.

10. McCarthy S, Das S, Kretzschmar W, et al. A reference panel of 64,976 haplotypes for genotype imputation. Nat Genet 2016;48(10):1279–83.

11. Auton A, Abecasis GR, Altshuler DM, et al. A global reference for human genetic variation. Nature 2015;526(7571):68–74.

12. Browning SR, Browning BL. Rapid and accurate haplotype phasing and missing-data inference for whole-genome association studies by use of localized haplotype clustering. Am J Hum Genet 2007;81(5):1084–97.

13. Browning BL, Zhou Y, Browning SR. A One-Penny Imputed Genome from Next-Generation Reference Panels. Am J Hum Genet 2018;103(3):338–48.

14. Zhou X, Stephens M. Genome-wide efficient mixed-model analysis for association studies. Nat Genet 2012;44(7):821–4.

15. Mägi R, Morris AP. GWAMA : software for genome-wide association meta-analysis. BMC Bioinformatics 2010;11(288):1–6.

16. R Core Team. R: a language and environment for statistical computing [Internet]. R Found. Stat. Comput. Vienna, Austria. 2015;Available from: http://www.r-project.org/

17. Pouw RB, Brouwer MC, Geissler J, et al. Complement factor H-related protein 3 serum levels are low compared to factor H and mainly determined by gene copy number variation in CFHR3. PLoS One 2016;11(3):e0152164.

18. Ward LD, Kellis M. HaploReg: A resource for exploring chromatin states, conservation, and regulatory motif alterations within sets of genetically linked variants. Nucleic Acids Res 2012;40(D):D930–4.

19. Ang LT, Tan AKY, Autio MI, et al. A Roadmap for Human Liver Differentiation from Pluripotent Stem Cells. Cell Rep 2018;22(8):2190–205.

20. Hathaway NA, Bell O, Hodges C, Miller EL, Neel DS, Crabtree GR. Dynamics and memory of heterochromatin in living cells. Cell 2012;149(7):1447–60.

21. Cong L, Ran FA, Cox D, et al. Multiplex genome engineering using CRIPRS/Cas systems. Science (80-) 2013;339(6121):819–23.

22. Mashiko D, Fujihara Y, Satouh Y, Miyata H, Isotani A, Ikawa M. Generation of mutant mice by pronuclear injection of circular plasmid expressing Cas9 and single guided RNA. Sci Rep 2013;3:3355.

23. Sun BB, Maranville JC, Peters JE, et al. Genomic atlas of the human plasma proteome. Nature 2018;558(7708):73–9.

Figure S1. - Overall study design

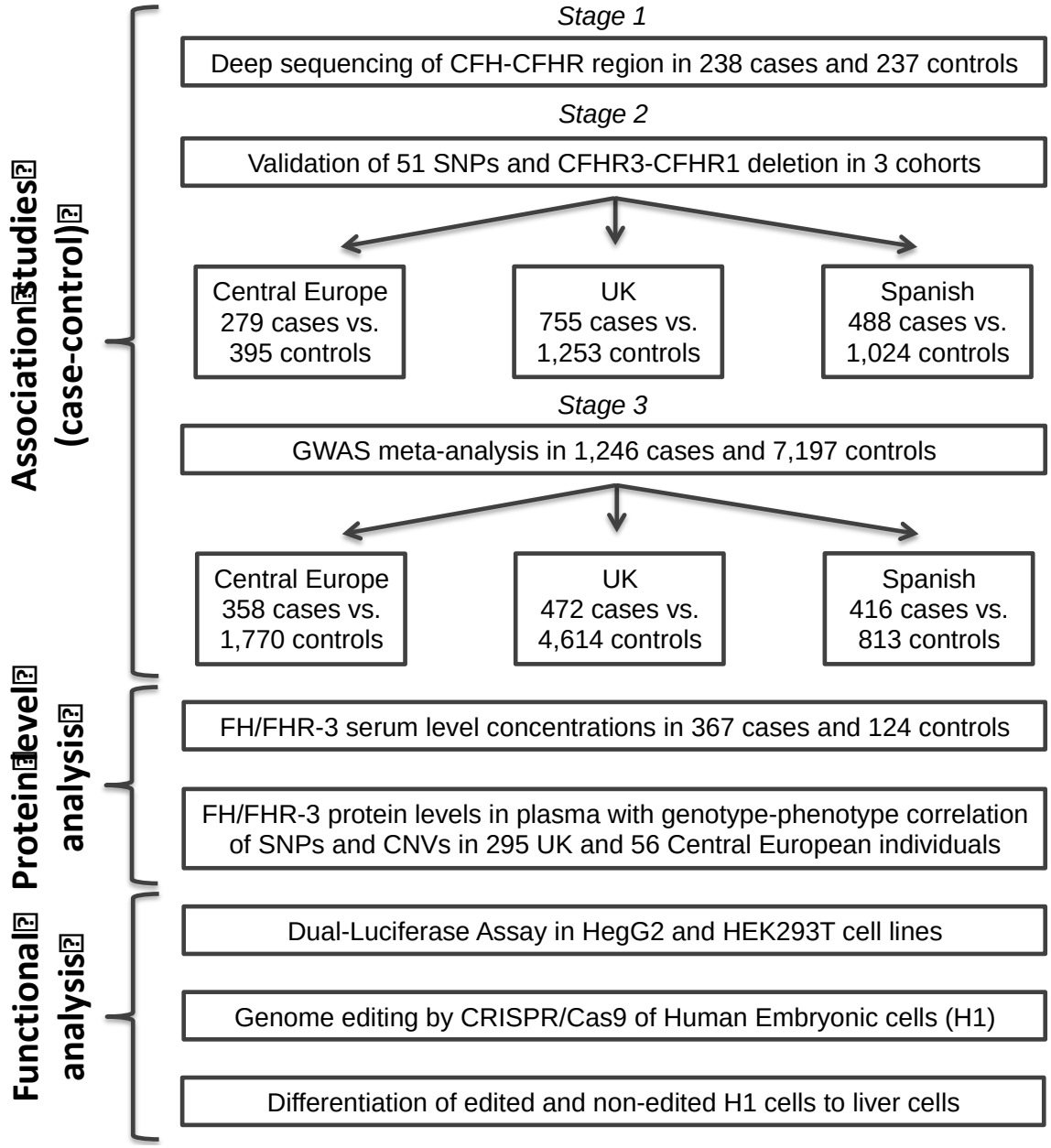

Figure S2. - Sequencing a) Target region (solid green) and captured region (chr1:196,620,000-196,979,000) including *CFH* to *CFHR5* genes. b) Depth of coverage of each samples (orange bars; average 227x ± 47) and percentage of sequenced region with depth of coverage 5x or more per sample (blue line)

A

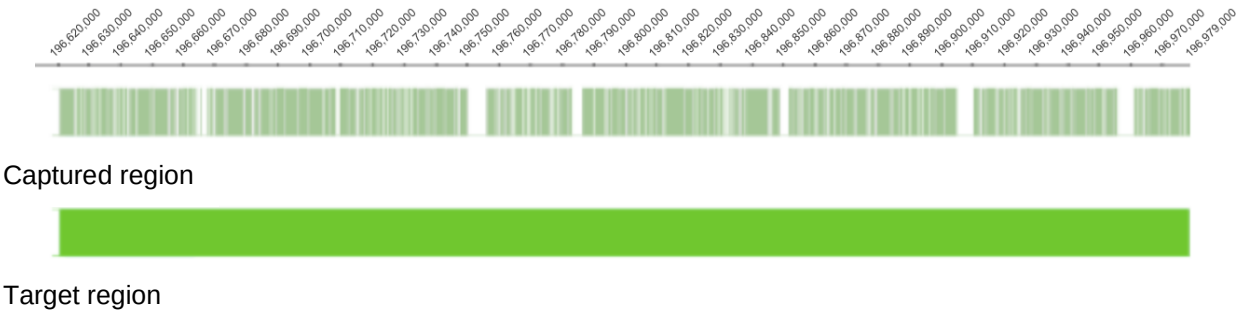

B

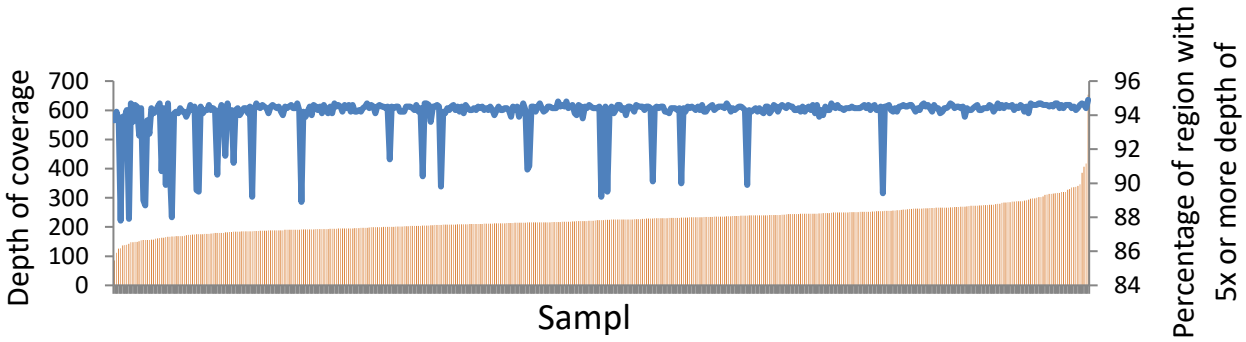

Figure S3. - Plot showing meta-analysis of quantitative trait association results based on samples without *CFHR3/CFHR1* deletions [combining the P-values, obtained by linear regression, of the UK (n=186) and the Central Europe (n=37) SNPs genotyped at the replication stage]. Genetic recombination rates (cM/Mb), estimated using 1KGP samples, are depicted by a blue line] and the color intensity of each symbol reflects the extent of LD with the labeled SNP rs75703017 (SNPs arranged according to their GRCh37/hg19 build chromosomal position on x-axis and genetic recombination rates (cM/Mb), estimated using 1KGP samples), for protein levels (µg/mL) of a) FH and b) FHR-3

A

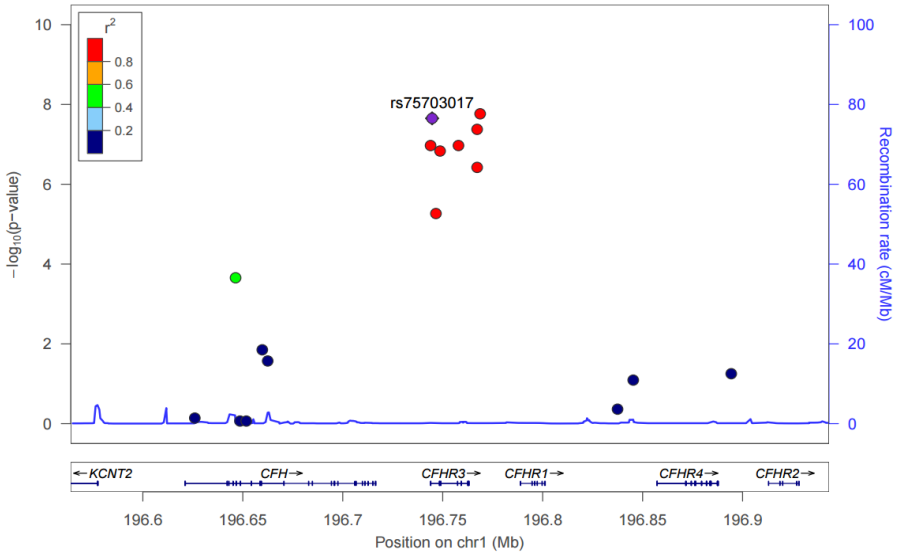

B

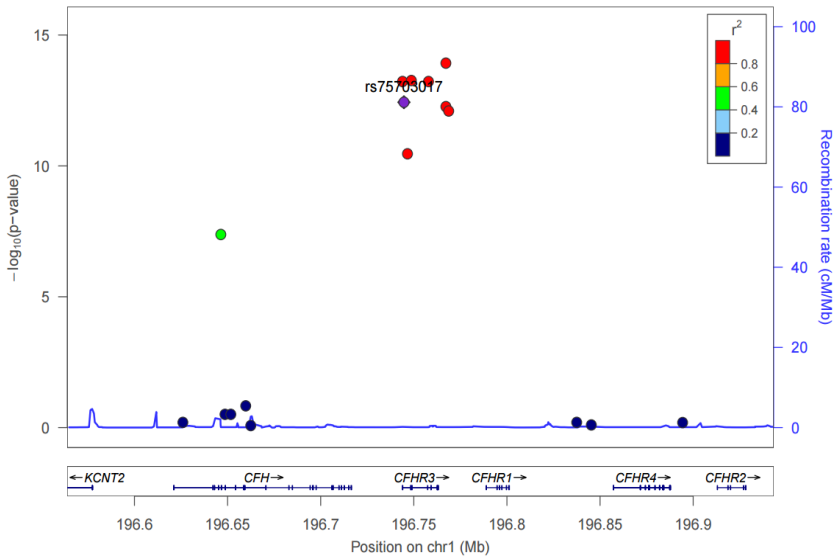

Figure S4. – a) Principal componant analysis (PCA). Plots showing the first 4 PCs of each single GWAS cohort A) CEC (red = CEC cases, green = Austrian and Dutch controls, blue = German controls); B) UK (red = UK cases, blue = UK controls); C) Spain (red = ESP cases, blue = ESP controls).

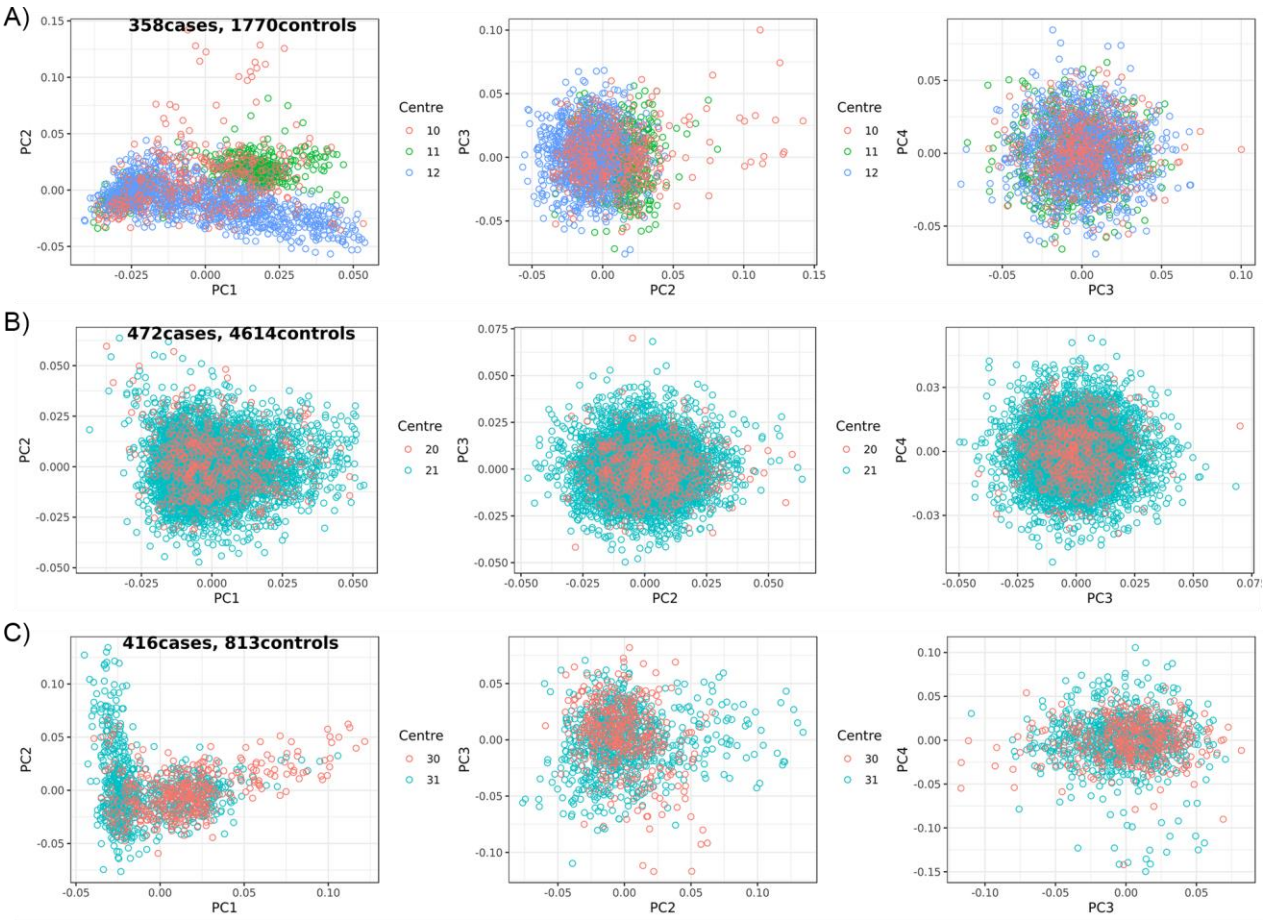

Figure S5. – Quantile-quantile (QQ) plot of the GWAS meta-analysis showing expected versus observed p-values calculated with R [chi <- (qchisq (1 - assoc$P, 1)) ; lambdaGC = median (chi) / qchisq (0.5, 1)] on genotyped variants only (298,246 intersecting variants, λ_{GC} = 1.007) and on all variants (6,387,059 variants, λ_{GC} = 1.002, figure not shown) as well as the LocusZoom online tool on a subset of genotyped and imputed variants (1,596,765 variants, λ_{GC} = 1.002, left upper and right lower corner).

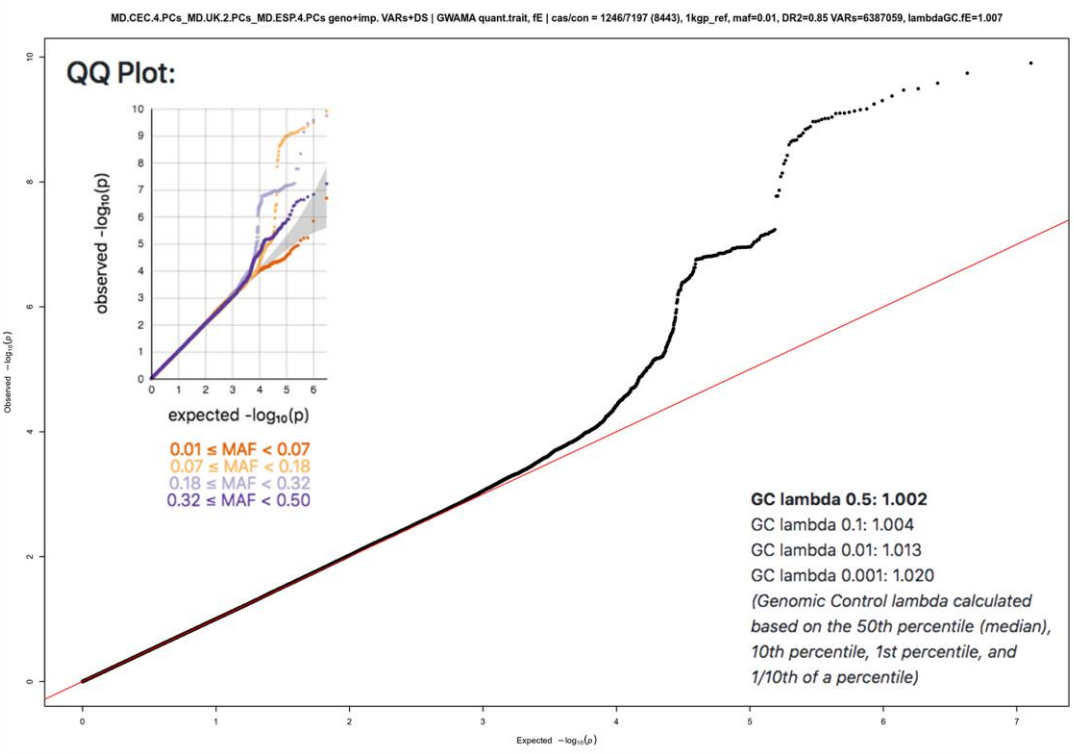

Figure S6. – Manhattan plot of the GWAS meta-analysis of genotyped (green dots shown below $1x10^{-3}$) and imputed variants. Autosmomes are shown on the x-axis and the observed p-values [-log10(p)] on the y-axis. Horizontal lines indicating the borders to suggestive (blue line; below $1x10^{-5}$) and genome-wide significant variants (red line; below $5x10^{-8}$).

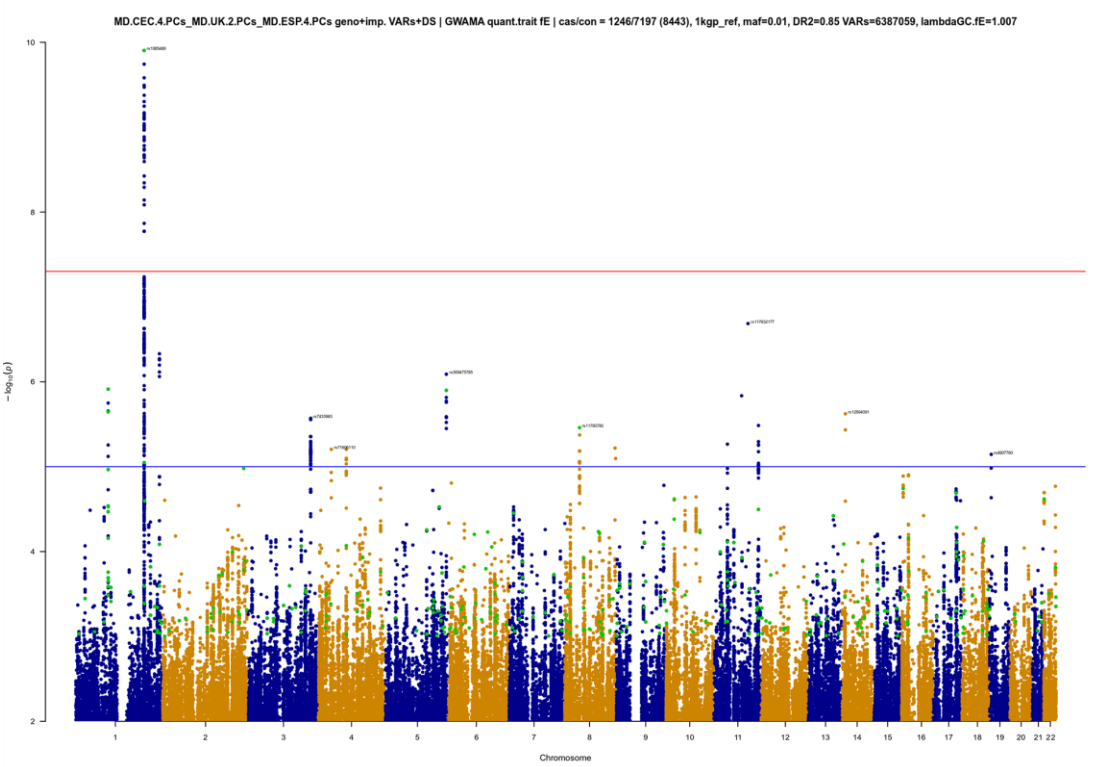

Figure S7. – a) Schematic illustration of the luciferase constructs used. Four test firefly plasmids pGL3-Empty, pGL3-C, pGL3-A & pGL3-AAC and the control renilla pRL-SV40 plasmid, each with key features and differences indicated. b) Effect of 2.8 kb regulatory sequence and the lead SNP rs75703017 (major and minor allele) on reporter (firefly luciferase) activity in HEK293T (Human embryonic kidney cell line). We compared cells containing an empty vector, mimicking CNV, (pGL3-Empty), and three constructs containing: major allele lead SNP, rs75703017 (pGL3-C); minor allele only (pGL3-A); and minor alleles of rs75703017and its two nearest SNPs (rs446868 and rs385390, pGL3-AAC). The graph is representative of five independent experiments.

A

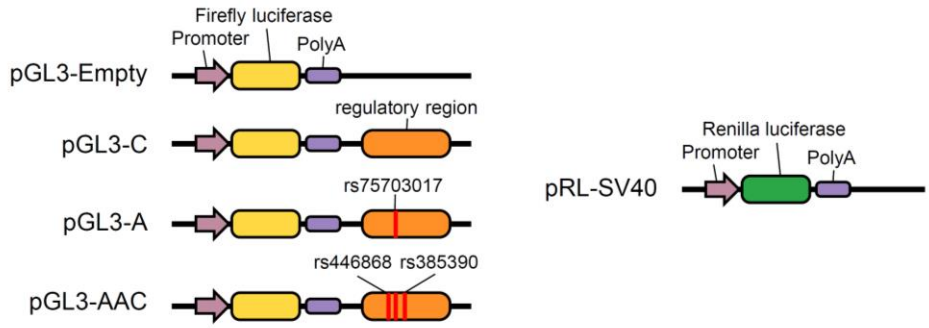

B

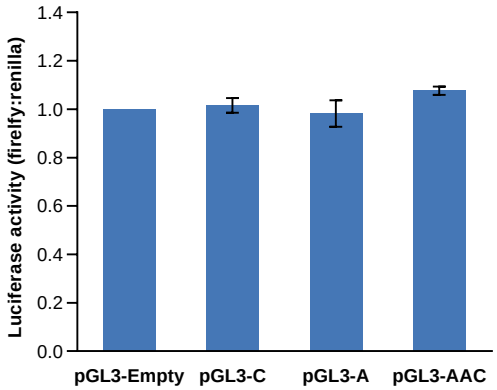

Figure S8. - a) Screening of CRISPR deleted clones. Lane 1: wild-type H1, lane 2: DNA ladder, lanes 3, 5 and 7: unsuccessful clones, lane 4: KO1(gRNA 1&3) and lane 6: KO2(gRNA 1-4). Expected size of wild type H1 is 3087bp b) Fold change [cells after liver differentiation (Diff)/undifferentiated (Undiff)] of expression levels for four liver markers of two CRISPR edited (KO) cell lines and one unedited (WT) H1 hES cell line (each colored bar for a protein represents one data point). Expression was measured by RT-qPCR.

A

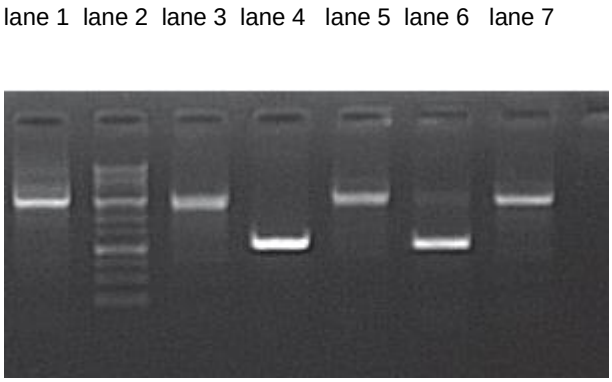

B

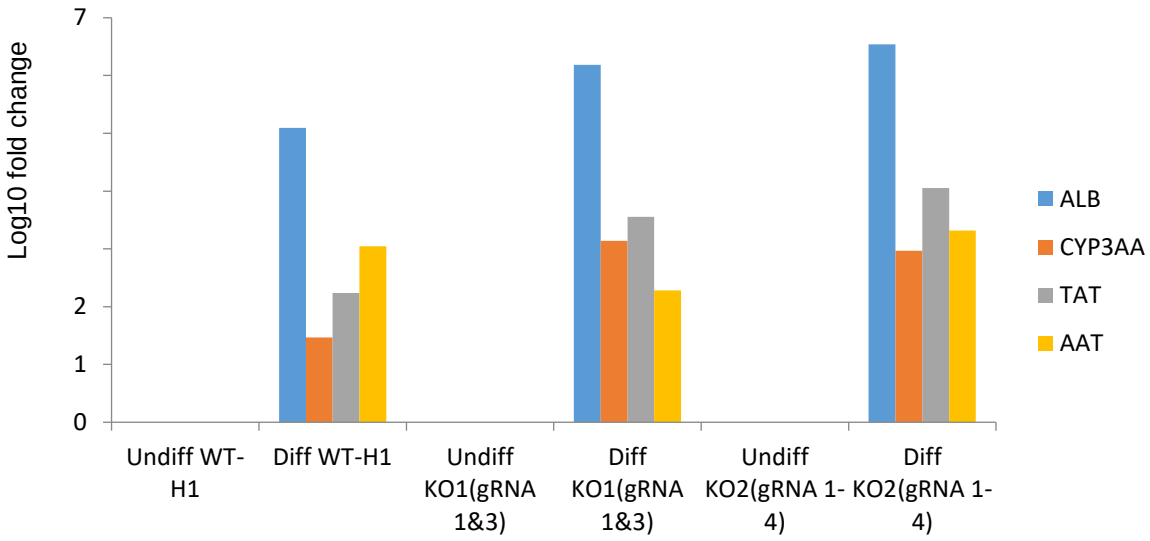

Figure S9. - Road Map ChIP-seq data (top panel) showing active regulatory region predicted only in the E066 liver cell-line by H3K4me3 (orange) and H3K9ac (purple) overlapping with the top SNP (rs75703017 depicted by yellow bar) and the SNPs in LD with it. UCSD Hi-C data (bottom panel) with 20 Kb resolution predicts cis-interaction (pink curves) between *CFHR3* and *CFH* gene in H1 and IMR90 cell lines. The 20 kb fragment showing this interaction includes intron 1 of *CFHR3*, location of rs75703017 (shadowed in yellow in the picture). For the purpose of reproducibility all the data were generated in duplicates.

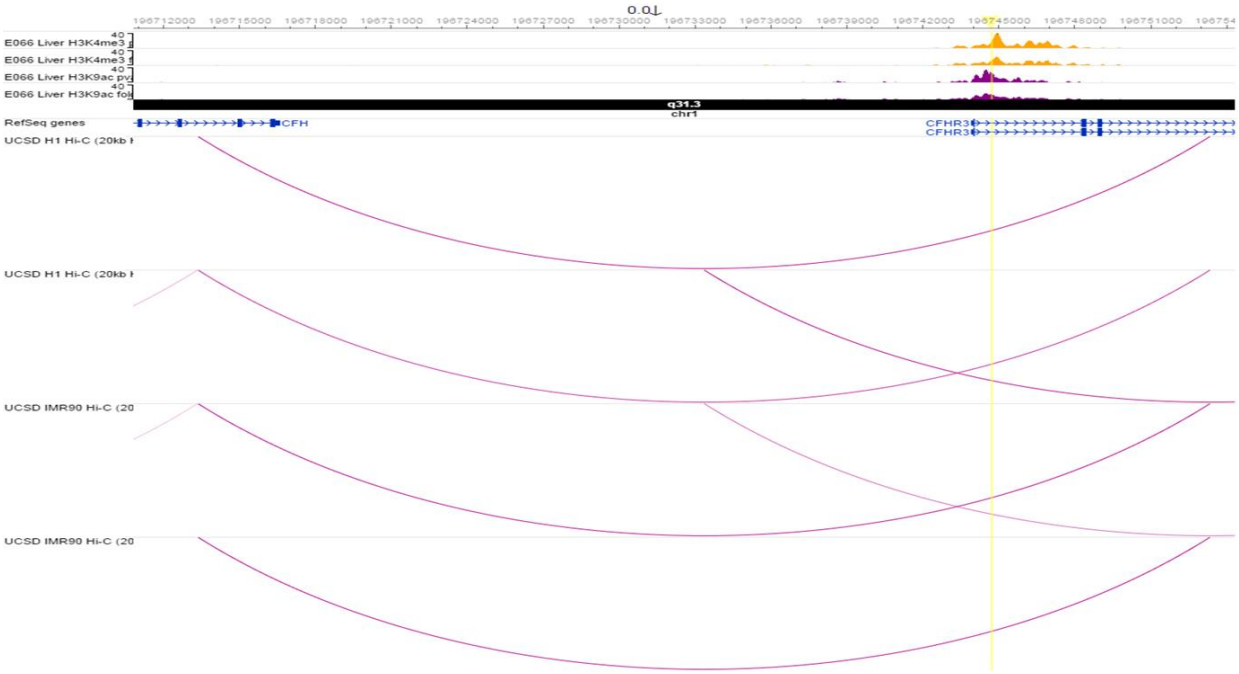

Table S1: Overall study design with methods and cohorts or cell lines

	Stage / Study	Cohorts	Platform / Method	Design	# Cases	# Ctrls	Cases vs Ctrls	Reference population / genetic coordinates	Notes
Association studies (case - control)	Initial GWAS (Davila et al. 2010)	UK	Illumina Human 610K + 1.2M	Discovery	475	4,703	1,480 vs 6,104	CEU HapMap population on GRCh36/hg18 coordiantes	Historical study; leadSNPs: rs1065489 (genotyped in CFH gene); rs426736 (imputed in CFHR3 gene); imputation in CFH/CFHR region only
		Western Europe	Sequenom Multiplex MassArray	Replication 1	590	864			
		Spain		Replication 2	415	537			
	First GWAS meta-analysis (Martinon-Torres et al. 2016)	Spain	Illumina Human 660W	Discovery	422	910	1,332 vs 5,178	EUR 1KGP phase 1 on GRCh37/hg19 coordiantes	Historical study; leadSNPs: rs1065489 (genotyped in CFH gene); rs193053835 (imputed in CFH gene); genome-wide imputation
		UK	Illumina Human 610K + 1.2M	Replication1	475	4,703			
	Stages 1 + 2 Fine-mapping by sequencing and genotyping	CEC	Nimblegen capture-targeted sequencing (HiSeq2000)	Discovery (stage 1)	238	237	1,760 vs 2,909	GRCh36/hg18 coordiantes	leadSNP: rs75703017 (sequenced and genotyped in CFHR3 gene)
		UK	Sequenom Multiplex MassArray	Replication (stage 2)	755	1,253			
		CEC			279	395			
		Spain			488	1,024			
	Detection of copy number variations (CNVs)	CEC from re-sequencing dataset	cnvCapSeq	Discovery	238	237	1,540 vs 1,700	GRCh36/hg18 coordiantes	-
			qPCR	Cross-validation	Subset of 67 from discovery				
			Taqman assay	Validation 2	1,302	1,463			
	Stages 3 Second GWAS meta-analysis	CEC	Illumina Human Omni 1M + Omni Express	Discovery	358	1,770	1,246 vs 7,197	1KGP phase 3 & HRC release v1.1 (subset) on GRCh37/hg19 coordiantes	leadSNPs: rs1065489 (genotyped in CFH gene); rs200384682 (InDel imputed in CFHR3 gene); rs431408 (SNP imputed in CFHR3 gene); genome-wide imputation
		UK	Illumina Human 610K + 1.2M	Replication 1	472	4,614			
		Spain	Illumina Human 660W	Replication 2	416	813			
Protein level analysis	FH/FHR-3 serum level concentrations	UK	ELISA	Discovery	308		367 vs 124	-	Case vs control comparison of FH and FHR-3 levels
		CEC			59	124			
	Protein quantitative trait loci (pQTL)	UK	ELISA, Multiplex ligation-dependent probe amplification (MLPA) & Taqman assays	Discovery	295		295 vs 56	-	Genotype-phenotype correlation of SNPs and CNVs for FH and FHR-3 levels
		CEC				56			
Functional analysis	Dual-Luciferase Assay	HepG2 (liver cell line)	Differential expression detected by a test reporter	Comparison of 4 different constructions: pGL3 (empty vector) vs pGL3-WT (wild type) vs pGL3-M (mutant alone) vs pGL3-3M (mutant + flanking SNPs)				-	-
		HEK293T (Kidney cell line)							
	Cell line differentiation	Human Embryonic cells (H1)	Genome-editing by CRISPR/Cas9	H1 cells were differentiated to liver with ability to express FH and FHR-3				-	-
	Stem cell differentiation to liver cells	edited H1 cells (genotype DD)	qRT-PCR	Fold change of CFH transcript expression levels in edited-H1 (DD) and non-edited H1 cells (DC) carrying 0 and 1 copy of CFHR3/CFHR1 genes, respesctively.				-	'D' = CFHR3/CFHR1 deletion and 'C' = wild type allele
		non-edited H1 cells (genotype DC)							

Table S2: Sequence of screening primers used to validate copy number variants within *CFHR1* and *CFHR3*

CFHR1 F:	AAATGCAGGTCCACTGGTAAGT
CFHR1 R:	GAGATGATGATGCTACCGGTTT
CFHR3 F:	GGAGAAAGGCTGGTCTCCTACT
CFHR3 R:	CTGAGACTGTCGTCCGTGTTAC

Table S3: Sequence of guided RNAs and screening primers used to target the region of interest

gRNA 1	GCTTCAATAATTCCAGTTAG
gRNA 2	CCTTAAAGCCCCTAGCTTCA
gRNA 3	AGCGTCCCAAAGAAGTACAA
gRNA 4	TTACACTTTGGCATAACAAA
Screening primer F	GAAGCCTTTCGTTCCCTT
Screening primer R	CACTAAAAGGCACTGGAA

Table S4: Number of SNPs which failed the different filtering criteria

	No of SNPs
Total	6020
PASS	4369
Strand Bias >60	733
Haplotype Score >13	249
Read Position Rank Sum <-8	354
Quality <50	144
MQ Rank Sum < -12.5	674
Quality by depth <2	539
Mapping Quality < 40	543

Table S5: List of SNPs genotyped by Sequenom on Chromosome 1 (n=44)

Variant ID	Position (GRCh37/hg19)
No reported SNP	196,633,739
rs34181066	196,643,762
rs72734328	196,667,944
rs12568400	196,738,295
rs385390	196,743,927
rs376841	196,746,600
rs425524	196,746,724
rs111994907	196,755,801
rs401188	196,757,083
rs387107	196,757,881
rs116249058	196,767,218
rs12409571	196,768,726
rs57426012	196,837,456
rs41310132	196,928,188
rs1329423	196,646,387
rs12127759	196,648,613
rs16840419	196,651,745
rs34331968	196,659,753
rs10922093	196,661,181
rs11580821	196,667,729
No reported SNP	196,701,018
rs1854499	196,737,289
rs75703017	196,744,699
rs620015	196,748,676
rs1738741	196,767,225
rs10754207	196,824,278
rs12240148	196,845,307
rs4086175	196,894,326
rs12134975	196,625,997
rs10922096	196,662,459
rs453912	196,737,303
rs2878713	196,739,431
rs11807686	196,739,564
rs12408446	196,741,197
rs11807997	196,743,213
rs370789	196,756,240
rs391537	196,756,615
rs390154	196,757,093
rs377298	196,758,541
rs1694442	196,767,289
rs532507	196,767,381
rs396051	196,776,342
No reported SNP	196,801,353
rs138307921	196,961,576

Table S6.- Comparison of notable GWAS variants from this study using the 1KGP controls, with GWAS and protein quantitative trait loci (pQTL) from Sun et al[23]. *dbSNP associated with MD[1].

GWAS SNPs	MD.1KGP P-value	Sun et al. P-value (GWAS or pQTL)	Disease or Target / Mapped Gene	Position on Chr 1
rs1065489	$1.25x10^{-10}$	NA	MD / CFH	196,709,774
rs529541	$1.30x10^{-09}$	$7.2x10^{-23}$	Factor H / CFH	196,719,716
rs6695321	$6.04x10^{-08}$	$2.6x10^{-27}$	PP2A, subunit B / CFH	196,675,861
rs75703017	$6.80x10^{-08}$	NA	MD / CFHR3	196,744,699
*rs426736	$1.12x10^{-07}$	NA	MD / CFHR3	196,760,417
rs1061170	$2.83x10^{-04}$	$1.0x10^{-261}$	Age-related macular deg. / CFH	196,659,237
rs35662416	$1.23x10^{-03}$	$3.8x10^{-121}$	PDGFRA / CFHR5	196,967,354
rs67908756	$1.26x10^{-02}$	$3.9x10^{-14}$	Calnexin / CFHR4	196,821,380
rs7519758	$1.56x10^{-02}$	$1.4x10^{-304}$	LRC19 / CFHR4	196,825,287
rs71631868	$4.06x10^{-02}$	$3.2x10^{-17}$	XRCC4 / CFHR4	196,815,711
rs1410996	$2.13x10^{-01}$	$0.0x10^{-00}$	Age-related macular deg. / CFH	196,696,933
rs2274700	$2.39x10^{-01}$	$1.6x10^{-51}$	Age-related macular deg. / CFH	196,682,947

Table S7.- Adjusted P-values estimated using the t-test between different genotype categories of rs75703017 for FHR-3 (lower triangle of the matrix) and FH levels (n=358) (upper triangle of the matrix, respectively). The P-value is adjusted for multiple comparison correction using Holm's method. The description of the alleles is in Figure 2.

	AA	CA	DA	CC	DC	DD
AA		0.82	0.45	0.04	4.8×10^{-3}	6.9×10^{-6}
CA	0.05		0.48	1.5×10^{-4}	2.7×10^{-7}	2.3×10^{-9}
DA	1.6×10^{-3}	0.04		0.82	0.44	2.1×10^{-3}
CC	4.8×10^{-7}	3.5×10^{-10}	0.32		0.18	1.1×10^{-4}
DC	5.8×10^{-13}	$<2.0 \times 10^{-16}$	1.4×10^{-3}	1.6×10^{-9}		6.8×10^{-3}
DD	7.6×10^{-16}	$<2.0 \times 10^{-16}$	7.4×10^{-7}	5.5×10^{-10}	2.2×10^{-3}	

Table S8.- Unadjusted Odds ratio (P-values) of the *CFHR3/CFHR1* deletion with susceptibility to MD.

Sequence	Replication			
Central European	Central European	UK	Spain	Meta Analysis
1.49 (0.028)	1.1 (0.50)	1.01 (0.94)	1.07 (0.50)	1.02 (0.76)

Table S9.- Unadjusted P-values for MD estimated using logistic regression analysis for top associated SNP (rs75703017). To eliminate the effect of risk allele 'C', only samples with mutant 'A' allele were considered. Dominant model refers to AA + A/del vs del/del comparison. 'del' refers to *CFHR3/CFHR1* deletion

	Genotypes			Total	P-Values	
	AA	A/del	del/del		Genotype model	Dominant model
Cases/Controls	35/50	69/140	73/78	177/268	0.013	8.10×10^{-3}

Table S11.- Beta and P-values for top associated SNP (rs75703017 with minor allele 'A') obtained using phenotype-genotype correlation from FH and FHR-3 protein dataset. To remove the effect of copy number change, samples without copy number change were considered (n=185 and 37 for the UK and the Central Europe samples, respectively) for the analysis.

	UK			Western Europe			Meta-Analysis			
	Beta	SE	P	Beta	SE	P	Beta	P	Q	I^2
FHR-3	0.4781	0.06926	8.11×10^{-11}	0.3887	0.1674	0.0262	0.465	3.70×10^{-13}	0.6217	0.00
FH	-47.46	9.135	5.41×10^{-07}	-69.1	31.8	0.03666	-49.1096	2.23×10^{-08}	0.5131	0.00

Table S12: Sequence of primers and oligos for plasmid construction

EF1a F	GACAAATGGCTCTAGATTCACTCGAGGTGCCCGT
EF1a R	TGAAAAAAAGTGATTATCCTCACGACACCTGAAA
Amp pUC F	GAATTTTAACAAAATTAGACGTCAGGTGGCACT
Amp pUC R	CTCGAGTGAATCTAGAATGTAACGGACCTCGAGC
sg chimeric pUC F	TCCGTTACATTCTAGGAGGGCCTATTTCCCATGA
sgRNA cassette F	GACAAATGGCTCTAGGAGGGCCTATTTCCCATGA
sgRNA cassette R	CTCGAGTGAATCTAGAGCCATTTGTCTGCAGAATTGG
Cas9 3' F	AGCTGCTGGGGATCACCATCATGGAAAGAAGCAGCTTCGAGAA
Cas9 3' 2sg R	AGTGGCTCCGCTTCCCTTTTTCTTTTTTGCCTGGCCGGCCTTT
Cas9 3' 4sg R	AGTGGCTCCGCTTCCGCTGGCCTCCACCTTTCTCT
2A Clover F	ggaagcggagccactaacttctccctgttgaaac
2A Clover R	CGAGCTCTAGGAATTCttaCTTGTACAGCTCGTCCAT
luci 5' F	gtaaaatcgataaggatccgCATTTTGTAAAACTCTCTGAAC
luci 5' R	atatagttctTTAATATGCAAGGCCTGC
luci 3' F	tgcatattaaAGAACTATATGGTAACATTAGCAG
luci 3' R	aaggctctcaagggcatcggAGTCAAGGAAATCCTGGG

Table S13: Sequences of primers used for qPCR for quantification of liver specific transcripts, *CFH* and *CFHR3* in H1 and H1-differentiated liver cells

Gene	Forward	Reverse
TAT	CCTTTACTTGGAAGGCTTCGCT	CGTCCAGAATTGAGGGGAGGTT
CYP3A4	AAGTGTGGGGCTTTTATGATGGT	GGTGAAGGTTGGAGACAGCAATG
AAT	CCCCTGTTTGCTCCTCCGATAA	CGGCATTGTCGATTCACTGTCC
ALB	ACCCCACACGCCTTTGGCACAA	CACACCCCTGGAATAAGCCGAGCT
CFH	TGCACAAGTACTGGCTGGAT	TCCCAGTAACTTCCTGACGGA

Funding supporting the establishment of MD cohorts used in this study

The UK meningococcal cohort was established with support from Meningitis Research Foundation through grants to Imperial College London (MRF 0402 and 1004.0). Patients were recruited through a grant from the Imperial College Biomedical Research Center (DMPED_P26077). The ESIGEM Research group activities were supported by grants from GePEM (Instituto de Salud Carlos III(ISCIII)/PI16/01478/Cofinanciado FEDER), DIAVIR (Instituto de Salud Carlos III(ISCIII)/DTS19/00049/Cofinanciado FEDER; Proyecto de Desarrollo Tecnológico en Salud), Resvi-Omics (Instituto de Salud Carlos III(ISCIII)/PI19/01039/Cofinanciado FEDER), BI-BACVIR (PRIS-3; Agencia de Conocimiento en Salud (ACIS)—Servicio Gallego de Salud (SERGAS)—Xunta de Galicia; Spain), Programa Traslaciona Covid-19 (ACIS—Servicio Gallego de Salud (SERGAS)—Xunta de Galicia; Spain) and Axencia Galega de Innovación (GAIN; IN607B 2020/08—Xunta de Galicia; Spain). (A.S.); Consellería de Sanidade, Xunta de Galicia (RHI07/2-intensificación actividad investigadora, PS09749 and 10PXIB918184PR), Instituto de Salud Carlos III (Intensificación de la actividad investigadora 2007–2016), Convenio de colaboración de investigación (Wyeth España-Fundación IDICHUS 2007–2011), Convenio de colaboración de investigación (Novartis España-Fundación IDICHUS 2010–2011), Fondo de Investigación Sanitaria (FIS; PI070069/PI1000540) del plan nacional de I + D + I and 'fondos FEDER' (F.M.T.). The Swiss Pediatric Sepsis study was funded by grants from the Swiss National Science Foundation (342730_153158/1 and 320030_201060/1), the Swiss Society of Intensive Care, the Bangerter Foundation, the Vinetum and Borer Foundation, and the Foundation for the Health of Children and Adolescents. The Central European Meningococcal Study was supported by grants no. 8842, 10112 and 12710 of the Oesterreichische Nationalbank (Austria), grants A3-16.K-8/2008-11 and A3-16.K-8/2006-9 of the Department for Science and Research of the Styrian federal government (Austria) and the non for profit association 'In Vita', Graz (Austria).

EUCLIDS consortium author list

Imperial College partner (UK)

Members of the EUCLIDS Consortium at Imperial College London (UK)

Principal and co-investigators

Michael Levin (grant application, EUCLIDS Coordinator)

Dr. Lachlan Coin (bioinformatics)

Stuart Gormley (clinical coordination)

Shea Hamilton (proteomics)

Jethro Herberg (grant application, PI)

Bernardo Hourmat (project management)

Clive Hoggart (statistical genomics)

Myrsini Kaforou (bioinformatics)

Vanessa Sancho-Shimizu (genetics)

Victoria Wright (grant application, scientific coordination)

Consortium members at Imperial College

Amina Abdulla

Paul Agapow

Maeve Bartlett

Evangelos Bellos

Hariklia Eleftherohorinou

Rachel Galassini

David Inwald

Meg Mashbat

Stefanie Menikou

Sobia Mustafa

Simon Nadel

Rahmeen Rahman

Clare Thakker

EUCLIDS UK Clinical Network

Poole Hospital NHS Foundation Trust, Poole: Dr S Bokhandi (PI), Sue Power, Heather Barham

Cambridge University Hospitals NHS Trust, Cambridge: Dr N Pathan (PI), Jenna Ridout, Deborah White, Sarah Thurston

University Hospital Southampton, Southampton: Prof S Faust (PI), Dr S Patel (co-investigator), Jenni McCorkell.

Nottingham University Hospital NHS Trust: Dr P Davies (PI), Lindsey Crate, Helen Navarra, Stephanie Carter

University Hospitals of Leicester NHS Trust, Leicester: Dr R Ramaiah (PI), Rekha Patel

Portsmouth Hospitals NHS Trust, London: Dr Catherine Tuffrey (PI), Andrew Gribbin, Sharon McCready

Great Ormond Street Hospital, London: Dr Mark Peters (PI), Katie Hardy, Fran Standing, Lauren O'Neill, Eugenia Abelake

King's College Hospital NHS Foundation Trust, London; Dr Akash Deep (PI), Eniola Nsirim

Oxford University Hospitals NHS Foundation Trust, Oxford Prof A Pollard (PI), Louise Willis, Zoe Young

Kettering General Hospital NHS Foundation Trust, Kettering: Dr C Royad (PI), Sonia White

Central Manchester NHS Trust, Manchester: Dr PM Fortune (PI), Phil Hudnott

SERGAS Partner (Spain)

Principal Investigators

Federico Martinón-Torres[1]

Antonio Salas[1,2]

GENVIP RESEARCH GROUP (in alphabetical order):

Fernando Álvez González[1], Ruth Barral-Arca[1,2], Miriam Cebey-López[1], María José Curras-Tuala[1,2], Natalia García[1], Luisa García Vicente[1], Alberto Gómez-Carballa[1,2], Jose Gómez Rial[1], Andrea Grela Beiroa[1], Antonio Justicia Grande[1], Pilar Leboráns Iglesias[1], Alba Elena Martínez Santos[1], Federico Martinón-Torres[1], Nazareth Martinón-Torres[1], José María Martinón Sánchez[1], Belén Mosquera Pérez[1], Pablo Obando Pacheco[1], Jacobo Pardo-Seco[1,2], Sara Pischedda[1,2], Irene Rivero Calle[1], Carmen Rodríguez-Tenreiro[1], Lorenzo Redondo-Collazo[1], Antonio Salas[1,2], Sonia Serén Fernández[1], María del Sol Porto Silva[1], Ana Vega[1,3].

[1] Translational Pediatrics and Infectious Diseases, Pediatrics Department, Hospital Clínico Universitario de Santiago, Santiago de Compostela, Spain, and GENVIP Research Group (www.genvip.org), Instituto de Investigación Sanitaria de Santiago, Galicia, Spain.

[2] Unidade de Xenética, Departamento de Anatomía Patolóxica e Ciencias Forenses, Instituto de Ciencias Forenses, Facultade de Medicina, Universidade de Santiago de Compostela, and GenPop

Research Group, Instituto de Investigaciones Sanitarias (IDIS), Hospital Clínico Universitario de Santiago, Galicia, Spain

[3] Fundación Pública Galega de Medicina Xenómica, Servizo Galego de Saúde (SERGAS), Instituto de Investigaciones Sanitarias (IDIS), and Grupo de Medicina Xenómica, Centro de Investigación Biomédica en Red de Enfermedades Raras (CIBERER), Universidade de Santiago de Compostela (USC), Santiago de Compostela, Spain

EUCLIDS SPANISH CLINICAL NETWORK:

Susana Beatriz Reyes[1], María Cruz León León[1], Álvaro Navarro Mingorance[1], Xavier Gabaldó Barrios[1], Eider Oñate Vergara[2], Andrés Concha Torre[3], Ana Vivanco[3], Reyes Fernández[3], Francisco Giménez Sánchez[4], Miguel Sánchez Forte[4], Pablo Rojo[5], J.Ruiz Contreras[5], Alba Palacios[5], Marisa Navarro[6], Cristina Álvarez Álvarez[6], María José Lozano[6], Eduardo Carreras[7], Sonia Brió Sanagustín[7], Olaf Neth[8], Mª del Carmen Martínez Padilla[9], Luis Manuel Prieto Tato[10], Sara Guillén[10], Laura Fernández Silveira[11], David Moreno[12].

[1] Hospital Clínico Universitario Virgen de la Arrixaca; Murcia, Spain.

[2] Hospital de Donostia; San Sebastián, Spain.

[3] Hospital Universitario Central de Asturias; Asturias, Spain.

[4] Complejo Hospitalario Torrecárdenas; Almería, Spain.

[5] Hospital Universitario 12 de Octubre; Madrid, Spain.

[6] Hospital General Universitario Gregorio Marañón; Madrid, Spain.

[7] Hospital de la Santa Creu i Sant Pau; Barcelona, Spain.

[8] Hospital Universitario Virgen del Rocío; Sevilla, Spain.

[9] Complejo Hospitalario de Jaén; Jaén, Spain.

[10] Hospital Universitario de Getafe; Madrid, Spain.

[11] Hospital Universitario y Politécnico de La Fe; Valencia, Spain.

[12] Hospital Regional Universitario Carlos Haya; Málaga, Spain.

FUNDING:

Instituto de Salud Carlos III (Proyecto de Investigación en Salud, Acción Estratégica en Salud: proyecto GePEM PI16/01478) (A.S.); Consellería de Sanidade, Xunta de Galicia (RHI07/2-intensificación actividad investigadora, PS09749 and 10PXIB918184PR), Instituto de Salud Carlos III (Intensificación de la actividad investigadora 2007–2016), Convenio de colaboración de investigación (Wyeth España-Fundación IDICHUS 2007–2011), Convenio de colaboración de investigación (Novartis España-Fundación IDICHUS 2010–2011), Fondo de Investigación Sanitaria (FIS; PI070069/PI1000540) del plan nacional de I + D + I and 'fondos FEDER' (F.M.T.).

Members of the Pediatric Dutch Bacterial Infection Genetics (PeD-BIG) network (the Netherlands)

Steering committee:

Coordination: R. de Groot [1], A.M. Tutu van Furth [2], M. van der Flier [1,4,46]

Coordination Intensive Care: N.P. Boeddha [3], G.J.A. Driessen [3,47], M. Emonts [3], J.A. Hazelzet [3]

Other members: T.W. Kuijpers [5], D. Pajkrt [5], E.A.M. Sanders [4] , D. van de Beek [6], A. van der Ende [6]

Trial coordinator: H.L.A. Philipsen [1]

Local investigators (in alphabetical order)

A.O.A. Adeel [7], M.A. Breukels [8], D.M.C. Brinkman [9], C.C.M.M. de Korte [10], E. de Vries [11], W.J. de Waal [12], R. Dekkers [13], A. Dings-Lammertink [14], R.A. Doedens [15], A.E. Donker [16], M. Dousma[17], T.E. Faber [18], G.P.J.M. Gerrits[19], J.A.M. Gerver [20], J. Heidema [21], J. Homan-van der Veen [22], M.A.M. Jacobs [23], N.J.G. Jansen [4], P. Kawczynski [24], K. Klucovska [25], M.C.J. Kneyber [26], Y. Koopman-Keemink [27], V.J. Langenhorst [28], J. Leusink [29], B.F. Loza [30], I.T. Merth [31], C.J. Miedema [32], C. Neeleman [1], J.G. Noordzij [33], C.C. Obihara [34], A.L.T. van Overbeek – van Gils [35], G.H. Poortman [36],S.T. Potgieter [37], J. Potjewijd [38], P.P.R. Rosias [39], T. Sprong [19], G.W. ten Tussher [40], B.J. Thio [41], G.A. Tramper-Stranders [42], M. van Deuren [1], H. van der Meer [2], A.J.M. van Kuppevelt [43], A.M. van Wermeskerken [44], W.A. Verwijs [45], T.F.W. Wolfs [4].

1. Radboud University Medical Center – Amalia Children's Hospital, Nijmegen, The Netherlands
2. Vrije Universiteit University Medical Center, Amsterdam, The Netherlands
3. Erasmus Medical Center – Sophia Children's Hospital, Rotterdam, The Netherlands
4. University Medical Center Utrecht – Wilhelmina Children's Hospital, Utrecht, The Netherlands

5. Academic Medical Center – Emma Children's Hospital, University of Amsterdam, Amsterdam, The Netherlands
6. Academic Medical Center, University of Amsterdam, Amsterdam, The Netherlands
7. Kennemer Gasthuis, Haarlem, The Netherlands
8. Elkerliek Hospital, Helmond, The Netherlands
9. Alrijne Hospital, Leiderdorp, The Netherlands
10. Beatrix Hospital, Gorinchem, The Netherlands
11. Jeroen Bosch Hospital, 's-Hertogenbosch, The Netherlands
12. Diakonessenhuis, Utrecht, The Netherlands
13. Maasziekenhuis Pantein, Boxmeer, The Netherlands
14. Gelre Hospitals, Zutphen, The Netherlands
15. Martini Hospital, Groningen, The Netherlands
16. Maxima Medical Center, Veldhoven, The Netherlands
17. Gemini Hospital, Den Helder, The Netherlands
18. Medical Center Leeuwarden, Leeuwarden, The Netherlands
19. Canisius-Wilhelmina Hospital, Nijmegen, The Netherlands
20. Rode Kruis Hospital, Beverwijk, The Netherlands
21. St. Antonius Hospital, Nieuwegein, The Netherlands
22. Deventer Hospital, Deventer, The Netherlands
23. Slingeland Hospital, Doetinchem, The Netherlands
24. Refaja Hospital, Stadskanaal, The Netherlands
25. Bethesda Hospital, Hoogeveen, The Netherlands

26. University Medical Center Groningen, Beatrix Children's hospital, Groningen, The Netherlands
27. Haga Hospital – Juliana Children's Hospital, Den Haag, The Netherlands
28. Isala Hospital, Zwolle, The Netherlands
29. Bernhoven Hospital, Uden, The Netherlands
30. VieCuri Medical Center, Venlo, The Netherlands
31. Ziekenhuisgroep Twente, Almelo-Hengelo, The Netherlands
32. Catharina Hospital, Eindhoven, The Netherlands
33. Reinier de Graaf Gasthuis, Delft, The Netherlands
34. ETZ Elisabeth, Tilburg, The Netherlands
35. Scheper Hospital, Emmen, The Netherlands
36. St. Jansdal Hospital, Hardewijk, The Netherlands
37. Laurentius Hospital, Roermond, The Netherlands
38. Isala Diaconessenhuis, Meppel, The Netherlands
39. Zuyderland Medical Center, Sittard-Geleen, The Netherlands
40. Westfriesgasthuis, Hoorn, The Netherlands
41. Medisch Spectrum Twente, Enschede, The Netherlands
42. St. Franciscus Gasthuis, Rotterdam, The Netherlands
43. Streekziekenhuis Koningin Beatrix, Winterswijk, The Netherlands
44. Flevo Hospital, Almere, The Netherlands
45. Zuwe Hofpoort Hospital, Woerden, The Netherlands

[46.] Section Paediatric Infectious Diseases, Laboratory of Medical Immunology, Radboud Institute for Molecular Life Sciences, Nijmegen, the Netherlands

[47.] Department of Paediatrics, Maastricht University Medical Center, Maastricht, The Netherlands

Swiss Pediatric Sepsis Study

Steering Committee:

Philipp KA Agyeman, MD [1], Christoph Berger, MD [2] , Christoph Aebi, MD [1], Luregn J Schlapbach, MD, FCICM [12,13]

Coinvestigators:

Philipp KA Agyeman, MD [1], Christoph Berger, MD [2] , Eric Giannoni, MD [3,4], Martin Stocker, MD [5], Klara M Posfay-Barbe, MD [6], Ulrich Heininger, MD [7], Sara Bernhard-Stirnemann, MD [8], Anita Niederer-Loher, MD [9], Christian Kahlert, MD [9], Giancarlo Natalucci, MD [10], Christa Relly, MD[2], Thomas Riedel, MD [1,11], Christoph Aebi, MD [1], Luregn J Schlapbach, MD, FCICM [12,13] **for the Swiss Pediatric Sepsis Study**

Affiliations:

[1] Department of Pediatrics, Inselspital, Bern University Hospital, University of Bern, Switzerland

[2] Division of Infectious Diseases and Hospital Epidemiology, and Children's Research Center, University Children's Hospital Zurich, Switzerland

[3] Clinic of Neonatology, Department Mother-Woman-Child, Lausanne University Hospital and University of Lausanne, Switzerland

[4] Infectious Diseases Service, Department of Medicine, Lausanne University Hospital and University of Lausanne, Switzerland

[5] Department of Pediatrics, Children's Hospital Lucerne, Lucerne, Switzerland

[6] Pediatric Infectious Diseases Unit, Children's Hospital of Geneva, University Hospitals of Geneva, Geneva, Switzerland

[7] Infectious Diseases and Vaccinology, University of Basel Children's Hospital, Basel, Switzerland

[8] Children's Hospital Aarau, Aarau, Switzerland

[9] Division of Infectious Diseases and Hospital Epidemiology, Children's Hospital of Eastern Switzerland St. Gallen, St. Gallen, Switzerland

[10] Department of Neonatology, University Hospital Zurich, Zurich, Switzerland

[11] Children's Hospital Chur, Chur, Switzerland

[12] Department of Intensive Care and Neonatology, and Children's Research Center, University Children's Hospital Zurich, Zurich, Switzerland

[13] Child Health Research Centre, The University of Queensland, and Paediatric Intensive Care Unit, Queensland Children's Hospital, Brisbane, Australia

Funding

This study was funded by grants from the Swiss National Science Foundation (342730_153158/1 and 320030_201060/1), the Swiss Society of Intensive Care, the Bangerter Foundation, the Vinetum and Borer Foundation, and the Foundation for the Health of Children and Adolescents.

Liverpool Partner

Principal Investigators

Enitan Carrol[1]

Stéphane Paulus [2]

ALDER HEY SERIOUS PAEDITRIC INFECTION RESEARCH GROUP (ASPIRE) (in alphabetical order):

Hannah Frederick[3], Rebecca Jennings[3] , Joanne Johnston[3], Rhian Kenwright[3]

[1] Department of Clinical Infection, Microbiology and Immunology, University of Liverpool Institute of Infection, Veterinary and Ecological Sciences , Liverpool, England

[2] Alder Hey Children's Hospital, Department of Infectious Diseases, Eaton Road, Liverpool, L12 2AP

[3] Alder Hey Children's Hospital, Clinical Research Business Unit, Eaton Road, Liverpool, L12 2AP

Micropathology Ltd

Colin G Fink[1,2], Elli Pinnock[1]

[1]Micropathology Ltd Research and Diagnosis

[2]University of Warwick

Newcastle partner

Principle Investigator

Marieke Emonts[1,2,3]

Co-Investigator

Rachel Agbeko[1,4]

[1] Translational and Clinical Research Institute, Newcastle University, Newcastle upon Tyne, United Kingdom

[2] Paediatric Infectious Diseases and Immunology Department, Newcastle upon Tyne Hospitals Foundation Trust, Great North Children's Hospital, Newcastle upon Tyne, United Kingdom

[3] NIHR Newcastle Biomedical Research Centre based at Newcastle upon Tyne Hospitals NHS Trust and Newcastle University, Westgate Rd, Newcastle upon Tyne, United Kingdom

[4] Paediatric Intensive Care Unit, Newcastle upon Tyne Hospitals Foundation Trust, Great North Children's Hospital, Newcastle upon Tyne, United Kingdom

Gambia partner

Suzanne Anderson: Principal Investigator and West African study oversight:

Fatou Secka: Clinical research fellow and study co-ordinator

Additional Gambia site team (consortium members):

Kalifa Bojang: co-PI

Isatou Sarr: Senior laboratory technician

Ngane Kebbeh: Junior laboratory technician

Gibbi Sey: lead research nurse Medical Research Council Clinic

Momodou Saidykhan: lead research nurse Edward Francis Small Teaching Hospital

Fatoumatta Cole: Data manager

Gilleh Thomas: Data manager

Martin Antonio: Local collaborator

Medical Research Council Unit Gambia

PO Box 273

Banjul

The Gambia

Members of the Central European Meningococcal Study Group

Principal Investigators: Alexander Binder[1], Werner Zenz[1]

Control Group: Wolfgang Walcher[2]

Central European Meningococcal Study Research Group (in alphabetical order): Alexander Binder[1], Gotho Geishofer[1], Daniela Kohlfürst[1], Müller Martin[1], Klaus Pfurtscheller[1], Karl Reiter[3], Siegfried Rödl[1], Werner Zenz[1], Gerfried Zobel[1], Bettina Zöhrer[1]

Additional Investigators Participating in the Central European Meningococcal Study Group: Bärbel Töpke [3], Peter Fucik [4], Markwart Gabriel [5], Johann M. Penzien [6], Gedeon Diab [7], Robert Miething [8], K.H. Deeg [9], Jürg Hammer [10], Ulrich Heininger [11], Verena Varnholt [12], Andreas Schmidt [13], Lutz Bindl [14], Ursula Sillaber [15], Christian Huemer [16], Primrose Meier [17], G. Simic-Schleicher [18], Markus Markart [19], Eberhard Pfau [20], Hans Broede [21], Bernd Ausserer [22], Hermann Kalhoff [23], Volker Arpe [24], Susanne Schweitzer-Krantz [25], Johannes-Martin Kasper [26], Kathrin Loranth [27], Hans J. Bittrich [28], Burkhard Simma [29], Jens Klinge [30], Michael Fedlmaier [31], Nicola

Weigand [32], Egbert Herting [33], Regina Grube [34], Christoph Fusch [35], Alois Gruber [36], Ulf Schimmel [37], Suzanne Knaufer-Schiefer [38], Wolfgang Lässig [39], Axel Hennenberger [40], Axel von der Wense [41], Roland Tillmann [42], Jürgen Schwarick [43], Friedrich C. Sitzmann [44], Werner Streif [45], Herbert Müller [46], Peter Kurnik [47], Peter Groneck [48], Ute Weiss [49], Helene Gröblacher-Roth [50], Jürgen Bensch [51], Reinhard Moser [52], Rudolf Schwarz [53], Kurt Lenz [54], Thomas Hofmann [55], Wolfgang Göpel [56], Dietrich Schulz [57], Thomas Berger [58], Erwin Hauser [59], Kai Martin Förster [60], Jochen Peters [61], Thomas Nicolai [62], Björn Kumlien [63], Regina Beckmann [64], Christiane Seitz [65], D. Hüseman [66], Roland Schürmann [67], Van Hop Ta [68], Eckart Weikmann [69], W. Evert [70], Jürgen Hautz [71], Jürgen Seidenberg [72], Lucia Wocko [73], Petra Luigs [74], Hans-Ludwig Reiter [75], J. Quietzach [76], Michael König [77], Johanna Herrmann [78], Horst Mitter [79], Ekkehard Seidler [80], Bernhard Maak [81], Wolfgang Sperl [82], Karl Zwiauer [83], Manfred Meissl [84], Reinhard Koch [85], Manfred Cremer [86], H.A. Breuer [87], W. Görke [88], Robert Nossal [89], Walter Pernice [90], Ralf Brangenberg [91], Hans R. Salzer [92], Hartmut Koch [93], Gerhard Schaller [94], Franz Paky [95], Friedrich Straßer [96], Franz Eitelberger [97], D. Sontheimer [98], Andreas Lischka [99], Martina Kronberger [100], Alfred Dilch [101], Christian Scheibenpflug [102], Robert Bruckner [103], Klaus Mahler [104], Klaus Runge [105], Wolfgang Kunze [106], Peter Schermann [107].

[1] Dept of General Pediatrics, Medical University of Graz, Graz

[2] Dept of Obstetics and Gynecology, Medical University of Graz, Graz

Kinderklinik der LMU München am Dr. von Haunerschen Kinderspital, Munich, Germany

[3] Ostalb-Klinikum, Aalen, Germany

[4] Krankenhaus Amstetten, Amstetten, Austria

[5] Klinikum Aschaffenburg, Aschaffenburg, Germany

[6] Zentralklinikum Kinderkliniken, Augsburg, Germany

[7] Kreiskrankenhaus Bad Hersfeld, Bad Hersfeld, Germany

[8] Diakonie-Krankenhaus, Bad Kreuznach, Germany

[9] Klinikum Bamberg, Bamberg, Germany

Universitäts-Kinderspital beider Basel, Pädiatrische Intensivmedizin, Basel,

[10] Switzerland

[11] Universitäts-Kinderspital beider Basel, Abt für Infektiologie, Basel, Switzerland

[12] Uni-Klinikum Charité, Campus Virchow Klinikum, Berlin, Germany

[13] St.-Agnes-Hospital, Bocholt, Germany

[14] Rheinische Friedrich-Wilhelms-Universität, Bonn, Germany

[15] Landeskrankenhaus Bregenz, Abt für Innere Medizin, Bregenz, Austria

[16] Landeskrankenhaus Bregenz, Abt für Kinderheilkunde, Bregenz, Austria

[17] Zentralkrankenhaus Links d. Weser, Bremen, Germany

[18] Zentralkrankenhaus Bremen-Nord, Bremen, Germany

[19] Ospedale di Bressanone, Brixen, Italy

[20] DRK-Krankenhaus Chemnitz-Rabenstein, Chemnitz, Germany

[21] Klinikum Lippe-Detmold GmbH, Detmold, Germany

[22] Krankenhaus Dornbirn, Dornbirn, Austria

[23] Städt. Kliniken Dortmund, Dortmund, Germany

[24] St. Marien-Hospital Düren-Birkesdorf, Düren, Germany

[25] Evangelisches Krankenhaus, Düsseldorf, Germany

[26] St. Georg Klinikum Eisenach gGmbH, Eisenach, Germany

[27] Krankenhaus der Barmherzigen Brüder, Eisenstadt, Austria

[28] Helios Klinikum Erfurt, Erfurt, Germany

[29] Landeskrankenhaus Feldkirch, Feldkirch, Austria

[30] Klinikum Fürth, Fürth, Germany

[31] Klinikum Garmisch-Partenkirchen, Garmisch-Partenkirchen, Germany

[32] Klinikum Justus-Liebig-Uni-O, Gießen, Germany

[33] Georg-August Universitäts-Kinderklinik, Göttingen, Germany

[34] Univ. Klinik für Neurologie, Graz, Austria

[35] Klinikum d. Ernst-Moritz-Arndt-Universität, Greifswald, Germany

[36] Krankenhaus der Schulschwestern Grieskirchen, Grieskirchen, Germany

[37] Allg. Krankenhaus Hagen GmbH, Hagen, Germany

[38] Ohrekreis-Klinikum, Haldensleben, Germany

[39] Städt. Krankenhaus Martha-Maria Halle-Dölau gGmbH, Halle, Germany

[40] Kinderkrankenhaus Wilhelmstift, Hamburg, Germany

[41] Altonaer Kinderkrankenhaus, Hamburg, Germany

[42] Klinikum Kreis Herford, Herford, Germany

[43] Kreiskrankenhaus Herzberg, Herzberg, Germany

[44] Univ. Klinik für Kinder- und Jugendmedizin, Homburg/Saar, Germany

[45] Univ. Klinik für Kinder- und Jugendheilkunde Innsbruck, Innsbruck, Austria

[46] Klinik Robert-Weixler-Strasse, Kempten, Germany

[47] Landeskrankenhaus Klagenfurt, Klagenfurt, Austria

[48] Kinderklinik der Stadt Köln, Köln, Germany

[49] Achenbach-Kreiskrankenhaus, Königs Wusterhausen, Germany

[50] Landeskrankenhaus Krems a. d. Donau, Krems a.d. Donau, Austria

[51] Vinzentius-Krankenhaus, Landau, Germany

[52] Landeskrankenhaus Leoben, Leoben, Austria

[53] Landes-Kinderklinik Linz, Linz, Austria

[54] Konventhospital der Barmherzigen Brüder, Linz, Austria

[55] Evangelisches Krankenhaus, Lippstadt, Germany

[56] Med. Universität zu Lübeck, Lübeck, Germany

[57] Städtisches Klinikum Lüneburg, Lüneburg, Germany

[58] Kantonspital Luzern, Luzern, Switzerland

[59] Landeskrankenhaus Mödling, Mödling, Austria

[60] Städt. Krankenhaus Harlaching, München, Germany

[61] Kinderklinik der TU München, München, Germany

[62] Kinderklinik im Dr. v. Haunerschen Kinderspital, München, Germany

[63] Kinderklinik des Dritten Ordens, München, Germany

[64] Dietrich-Bonhoeffer-Klinikum, Neubrandenburg, Germany

[65] FEK-Friedrich-Ebert-Krankenhaus. Neumünster GmbH, Neumünster, Germany

[66] Ruppiner Kliniken GmbH, Neuruppin, Germany

[67] Städt. Kliniken Neuss Lukaskrankenhaus GmbH, Neuss, Germany

[68] Evangelisches Krankenhaus, Oberhausen, Germany

[69] Landeskrankenhaus Oberwart, Oberwart, Austria

[70] Städt. Kliniken Offenbach, Offenbach, Germany

[71] Klinikum Offenburg, Offenburg, Germany

[72] Elisabeth-Kinderkrankenhaus, Oldenburg, Germany

[73] Krankenhaus Oranienburg, Oranienburg, Germany

[74] St.Vincenz-Krankenhaus Frauen- u. Kinderklinik, Paderborn, Germany

[75] Klinik für Kinder und Jugendliche am Städtischen Klinikum, Pforzheim, Germany

[76] Vogtland-Klinikum Plauen GmbH, Plauen, Germany

[77] Oberschwaben Klinik gGmbH, Ravensburg, Germany

[78] Kreiskrankenhaus Rendsburg, Rendsburg, Germany

[79] Krankenhaus der Barmherzigen Schwestern Ried, Ried i. Innkreis, Austria

[80] Kreiskrankenhaus Obergöltzsch-Rodewisch, Rodewisch, Germany

[81] Thüringen-Klinik “Georgius Agricola” gGmbH, Saalfeld, Germany

[82] Landeskrankenanstalten Salzburg, Salzburg, Austria

[83] Landesklinikum Sankt Pölten, Sankt Pölten, Austria

[84] Landeskrankenhaus Schärding, Schärding, Austria

[85] Leopoldina-Krankenhaus, Schweinfurt, Germany

[86] DRK-Kinderklinik Siegen, Siegen, Germany

[87] Städt. Klinikum Solingen, Solingen, Germany

[88] Johanniter Kinderklinik, Stendal, Germany

[89] Olga Hospital Stuttgart, Stuttgart, Germany

[90] Kreiskrankenhaus Torgau, Torgau, Germany

[91] Klinikum Traunstein, Traunstein, Germany

[92] Landeskrankenhaus Tulln, Tulln, Austria

[93] St. Marien-Hospital, Vechta, Germany

[94] Landeskrankenhaus Villach, Villach, Austria

[95] Landeskrankenhaus Vöcklabruck, Vöcklabruck, Austria

[96] Klinikum Weiden, Weiden, Germany

[97] Krankenhaus der Barmherzigen Schwestern v. heiligen Kreuz, Wels, Austria

[98] Harz-Klinikum Wernigerode GmbH, Wernigerode, Germany

[99] Wilhelminenspital Wien, Wien, Austria

[100] St. Anna Kinderspital, Wien, Austria

[101] Gottfried von Preyersches Kinderspital der Stadt Wien, Wien, Austria

[102] Donauspital im SMZ-Ost der Stadt Wien, Wien, Austria

[103] Krankenhaus Wiener Neustadt, Wiener Neustadt, Austria

[104] St. Elisabeth Krankenhaus, Wittlich, Germany

[105] Zentrum für Kinder- und Jugendmedizin, Wuppertal, Germany

[106] Krankenhaus Muldentalkreis Wurzen, Wurzen, Germany

[107] Krankenhaus Zwettl, Zwettl, Austria

Acknowledgements:

The Central Europe Meningococcal Study was supported by grants no 8842, 10112 and 12710 of the Oesterreichische Nationalbank (Austria), grants A3-16.K-8/2008-11 and A3-16.K-8/2006-

9 of the Department for Science and Research of the Styrian federal government (Austria) and the nonprofit association ‘In Vita’, Graz (Austria).